Sensitivity based continuation power flow

by

Srinivasu Battula

A Thesis Submitted to the

Graduate Faculty in Partial Fulfillment of the

Requirements for the Degree of

MASTER OF SCIENCE

Department: Electrical Engineering and Computer Engineering
Major: Electrical Engineering

Iowa State University
Ames, Iowa
1992

TABLE OF CONTENTS

LIST OF TABLES

LIST OF FIGURES

ACKNOWLEDGMENTS

I would like to thank my advisor Dr. V. Ajjarapu for his constant support and encouragement. I enjoyed working with him and he was always willing to help when I got stuck. Special thanks to Dr. John Lamont for reviewing my work and for his valuable suggestions. I would also like to thank Dr. Glenn Luecke for sparing his time to review my work.

Many thanks are also due to my parents, Prakasa Rao Battula and Malathi Battula, and my sister Sridevi, for their continued support and blessings, in all my endeavors. Finally, I would like to thank all my friends, especially Kishore Dhara and Vamsi Chadalavada, for their help and encouragement.

CHAPTER 1. INTRODUCTION

1.1 The Voltage Stability Problem

Society's dependency on electricity is increasing daily. To meet increased demand, generating facilities and major transmission lines must be built. During construction design, issues like delay of obtaining license to build new transmission lines from state agencies, difficulties in acquiring right-of-way from land owners, concerns regarding the relation of electromagnetic fields (EMF) to human health, and shift in generation pattern because of environmental constraints all come into play. The most feasible response is often to interconnect different utilities and to exchange power between them. Thus, modern electrical power systems tend to be highly interconnected and heavily loaded. As these systems continue to grow, voltage stability is becoming a major operating concern.

A system is said to enter a state of voltage instability when a disturbance (say an increased load) causes voltage to drop quickly and automatic system controls fail to halt the decay. Voltage decay may occur in only a few seconds or require 10 to 20 minutes. If the decay continues unabated, steady-state angular instability, or voltage collapse, occurs. In the literature, the voltage collapse point is generally referred as the critical point. This point is illustrated in figure 1.1, which plots the relation between real power and voltage at a load bus of a 2-bus system. The result is a

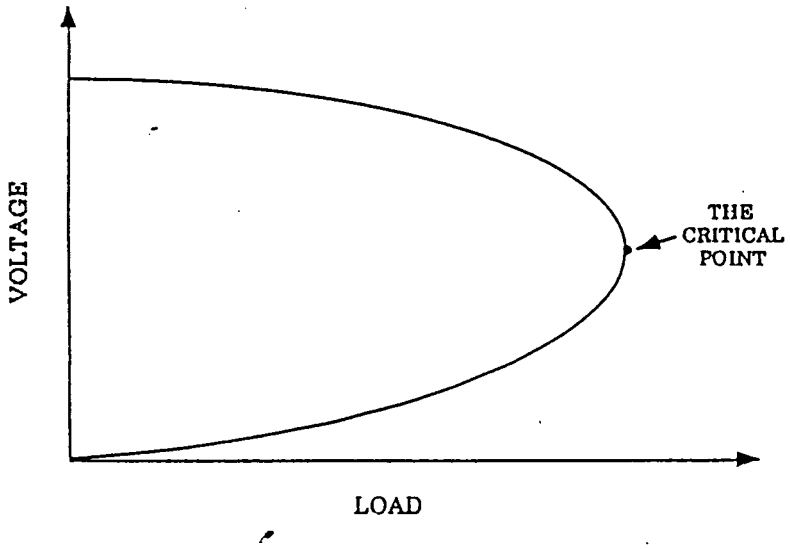

Figure 1.1: Illustration of the critical point on a P-V curve

P-V curve with the critical point located at the tip. The frequency of voltage collapse incidents has increased in recent years, involving millions of dollars in losses. To prevent recurrence, operators and planners must understand fully the voltage collapse phenomenon.

1.2 The Voltage Collapse Phenomenon

In a power system, if generation facilities are adjacent to load centers, real and reactive power can be supplied by generating units. But in many instances, generation facilities are remotely located. Thus, the need arises for compensation of the voltage drop along the transmission lines and for the provision of voltage support within the load areas. Items available to maintain the desired voltage and reactive flow levels under changing operating conditions include:

1. shunt capacitors,

2. under-load tap changing transformers (ULTCs),

3. static var compensators (SVCs),

4. shunt reactors, and

5. generator reactive power reserves.

In general, reactive power flows from a bus with a higher voltage magnitude to one with a lower voltage magnitude. An inductive reactive load lowers the voltage of the bus to which it is connected, whereas a capacitive reactive load raises the bus voltage.

As mentioned, the main problem is the voltage drop that occurs after a disturbance (an increase in load). Under such circumstances, excessive power because of increased loading, flows through inductive reactances of transmission lines and transformers. The problem is exacerbated if the reactive power supply at the local level is insufficient. But even when there is sufficient reactive power supply, if that supply is located far from the voltage-weak areas, it is of no use because reactive power cannot be transferred over great distances. The voltage decay problem becomes especially serious after a contingency, when cascading outages and voltage collapse throughout the system can result. Such voltage instability/collapse incidents that have occurred throughout the world are reported in [1].

One of the tools sometimes used for analyzing steady-state voltage stability is the Newton-Raphson power flow. But the Jacobian of the power flow becomes singular at the steady-state voltage limit, or the critical point. Consequently, the power flow equations cannot be solved at or near the critical point. This hampers the study of

voltage collapse. The next section briefly discusses the analytical and computational tools proposed by several researchers for analyzing the voltage stability problem.

1.3 Literature Review

In the literature, most of the static conditions derived to predict voltage instability can be related to singularity conditions on the power flow Jacobian. It should be noted, however, that the singularity of the power flow Jacobian is a necessary but not a sufficient condition to indicate voltage instability.

In any type of voltage stability analysis, we wish to know how close the system is to actual voltage instability, which can be expressed in terms of an index. Numerous such indices have been proposed to assess the proximity of an operating condition to voltage collapse. Tamura et al. [2, 3] related the voltage instability phenomenon to multiple power flow solutions. In a heavily loaded power system, two very close power flow solutions exist, that are called multiple power flow solutions. One is the higher-voltage power flow solution and the other is the lower-voltage solution. As the load demand increases, the two solutions approach each other, finally reaching the static voltage stability limit. Tiranuchit et al. [4] used the minimum singular value of the power flow Jacobian as a security index, and derived static control strategies based on this index. The minimum singular value zero corresponds to a singular Jacobian matrix. Kessel et al. [5] developed a local index, L_i, which is computed for each mode i in the system. The maximum value (closest to one) is indicative of the proximity to voltage instability, where the power flow solution diverges. Schlueter et al. [6] proposed the concept of PQ and PV controllability, and identified the voltage control areas by defining an area version of the minimum eigenvalue index.

As mentioned, a drawback common to all these methods is that they rely on the Newton-Raphson method of power flow analysis, which is unreliable in the vicinity of the voltage stability limit. To overcome such difficulties, new methods based on continuation and bifurcation are emerging. Iba et al. [7] applied the homotopy continuation method to detect the critical point. A homotopy parameter was introduced and used to trace without numerical ill-conditioning the solution along the curve from a base load to the critical load condition. This method is similar to the continuation method developed at Iowa State University (ISU) by means of predictor-corrector scheme [8].

1.4 Scope and Objective

In response to the need for a more robust and numerically well-conditioned analytical tool for analyzing steady-state voltage stability, a continuation power flow (CPF) program was developed at ISU [8].

The continuation power flow, which approximates the critical point, starts at a base load with a specified load change scenario. In one program run, it provides a series of power flow solutions up to and slightly past the critical point. For each power flow solution calculated, the CPF produces an index to identify the distance from the critical point and a list of buses most prone to voltage collapse. The present version of the CPF has been proved a powerful tool for approximating the critical point. However, the CPF provides no information with respect to identifying the system's weakest components from the voltage stability viewpoint. Moreover, the current CPF does not fully utilize the effect of load modeling on voltage stability.

The objective of this research is to make the available CPF a more powerful tool

for the analysis of steady-state voltage stability. This involves

- a detailed study of the various load models (constant power, constant current, constant impedance, and composite load models) to determine their effects on voltage stability;
- a definition of the concept load connectivity so as to clarify the understanding of the critical point with respect to PV curves; and
- a systematic procedure, identifying key components (buses, branches, and generators) of the system that are critical to maintaining voltage stability.

1.5 Thesis Outline

Chapter 2 describes the general principles involved in the analysis of steady-state voltage stability and provides robust numerical methods to be used in identifying voltage instability conditions. The basic principles involved in the CPF are reviewed in Chapter 3. In Chapter 4, the importance of load modeling in power systems (especially for voltage stability studies) is stressed, and the CPF is demonstrated with nonlinear load models. Chapter 5 presents a sensitivity approach using the tangent vector of continuation power flow to identify weak areas in the system. Chapter 6 contains both the conclusions drawn from this research and suggestions for future work.

CHAPTER 2. STEADY-STATE VOLTAGE STABILITY EVALUATION

2.1 Introduction

In this chapter, the basic definitions pertaining to voltage stability are given. The general principle of how steady-state voltage stability can be analyzed is outlined. Finally, the basic steps involved in the direct and indirect methods of calculating the critical point are presented.

2.2 Basic Definitions and Voltage Collapse Incidents

Throughout this research, the problem of voltage instability, which causes the voltage collapse phenomenon, is examined from the steady-state perspective. The accepted definition of the steady-state stability of a power system is as follows [9]:

"A power system is steady state stable for a particular steady state operating condition if, following any small disturbance, it reaches a steady state operating condition which is identical to or close to the pre-disturbance operating condition."

A small disturbance is defined as

"a disturbance for which the equations that describe the dynamics of the power system may be linearized for the sake of analysis."

In general, static voltage instability refers to the continuous decay of voltage to

Table 2.1: Voltage collapse incidents

Date	Location	Time Frame
11/30/86	SE Brazil, Paraguay	2 seconds
05/17/85	South Florida	4 seconds
08/22/87	Western Tennessee	10 seconds
12/27/83	Sweden	50 seconds
09/22/77	Jacksonville, Florida	few minutes
09/02/82	Florida	1-3 minutes
11/26/82	Florida	1-3 minutes
12/28/82	Florida	1-3 minutes
12/30/82	Florida	2 minutes
12/09/65	Brittany, France	?
11/10/76	Brittany, France	?
08/04/82	Belgium	4.5 minutes
01/12/87	Western France	4-6 minutes
07/23/87	Tokyo	20 minutes
12/19/78	France	26 minutes
08/22/70	Japan	30 minutes
12/01/87	France	?

a critical value causing the protection equipment to react and effectively separates the network. Loss of voltage control does not necessarily involve large or increasing angles. Disturbances involving voltage collapse have occurred over the last 20 years, the majority occurring since 1982. A number of incidents are listed in Table 2.1 [1]. The time frames for these types of disturbances range from a few seconds to thirty minutes or longer.

The need for a better understanding of the phenomenon and for exploring methods of analyzing and solving voltage stability problems led to the formation of an IEEE task force on the subject [10]. This task force developed a report containing part of the work published up to 1989. The report also proposed definitions for the

three local terms of the voltage control problem.

voltage stability: The ability of a system to maintain voltage so that when the load admittance is increased, load power will increase, so that both power and voltage are controllable

voltage collapse: The process by which voltage instability leads to loss of voltage in a significant part of the system (voltage may be lost due to angle instability as well, and sometimes only a careful post-incident analysis can discover the primary cause)

voltage security: The ability of a system not only to operate stably, but also to remain stable (as far as the maintenance of system voltage is concerned) following any reasonably credible contingency or adverse system change.

If, following a disturbance (such as a load increase or a change in system configuration), a rapid voltage drop occurs in the system and automatic system controls fail to halt decay, the power system is said to be insecure and to be in the state of voltage instability. If voltage continues to deteriorate, steady-state angular instability, or voltage collapse, will occur.

Growing concern about voltage collapse incidents around the world led to the organization of international workshops at the following places:

- Potosi, MO, September 1988;
- Deep Creek Lake, MD, August 1991;
- Lagos, Nigeria, January 1992; and

- EPRI/NERC forum on voltage stability, Breckenridge, CO, September 14-15, 1992.

2.3 Analysis of Steady-state Voltage Stability

The steady-state operation of a power system network is represented by the power flow equations given by

$$F(\underline{\delta}, \underline{V}, \lambda) = 0 \tag{2.1}$$

where $\underline{\delta}$ represents the vector of bus voltage angles, and $\underline{V}$ represents the vector of bus voltage magnitudes. λ is the parameter of interest we choose to vary. It can either be a load parameter in terms of MW or a load connection parameter, which will be explained in the following chapters. In general, the dimension of F will be $2n_{pq} + n_{pv}$, where n_{pq} and n_{pv} are the number of PQ and PV buses, respectively.

From equation 2.1 the fundamental equation of sensitivity analysis can be obtained as

$$dF = \frac{\partial F}{\partial \delta} d\delta + \frac{\partial F}{\partial V} dV + \frac{\partial F}{\partial \lambda} d\lambda = 0 \tag{2.2}$$

Let $x = [\underline{\delta}, \underline{V}]^T$. From the foregoing differential equation, an ODE system can be obtained:

$$\frac{dx}{d\lambda} = \left[\frac{\partial F}{\partial x}\right]^{-1} \frac{\partial F}{\partial \lambda} \tag{2.3}$$

For a specific variation of the parameter λ, the corresponding variation to solution x is calculated by evaluating the Jacobian $\partial F/\partial x$. This procedure, as proposed in Davidenko [11], fails at critical points where the Jacobian is singular and the inverse does not exist. At such points, the solution, x, is quite sensitive to even small parametric perturbations. In mathematical literature, these critical points are

referred to as turning points, limit points, or fold points.

Several techniques have been proposed to calculate turning points. These methods base their analyses on two approaches:

- direct methods [12, 13] and
- indirect methods [14, 15].

The former augments the original system of equations with an extra set of equations in such a way that the turning point becomes the solution of the system. The latter begins around the neighborhood of a turning point and calculates several different solutions of $F(x, \lambda) = 0$ by continuation. At the same time, a certain test function is monitored along the solution path, which gives information about the turning point. Both methods are described in the following sections. Excellent descriptions can be found in [16].

2.3.1 Direct methods

The first application of direct methods to power system problems is described by Ajjarapu [17] and Alvarado [18]. This approach attempts to find the maximum allowable variation of λ: i.e., an operating point $(\underline{x}^*, \lambda^*)$ of $F(\underline{x}, \lambda) = 0$, such that the Jacobian at this point is singular. It solves the system of equations

$$G(\underline{y}) = \begin{bmatrix} F(\underline{x}, \lambda) \\ F_x(\underline{x}, \lambda)\underline{h} \\ h_k - 1 \end{bmatrix} \tag{2.4}$$

This procedure basically augments the original power flow equations $F(\underline{x}, \lambda) = 0$ by $F_x(\underline{x}, \lambda)\underline{h} = 0$ with $h_k = 1$. This augmentation makes the Jacobian of the enlarged

system $G(y)$ nonsingular and guarantees a solution that is the turning point.

This approach has certain drawbacks. The dimension of the nonlinear set of equations to be solved is twice that of the conventional power flow. The approach requires close estimates for the vector $\underline{h}$. But convergence of the direct method is rapid if the initial operating point is close to the turning point. The enlarged system is solved in such a way that it requires the solution of four $n \times n$ (n is the dimension of the Jacobian $F_x(\underline{x}, \lambda)$) linear systems, each with the same matrix. Such a procedure requires only one LU decomposition. Details can be found in [12, 17]. A good comparison of the direct method with the continuation method is given in [19].

2.3.2 Indirect (continuation) methods

Unlike direct methods, which attempt to solve an enlarged system of load flow equations in one step, the continuation (indirect) method starts with a known base solution and attempts to solve the original load flow equations repeatedly. It assumes that the first solution (x_o, λ_o) of $F(x, \lambda) = 0$ is available. The continuation problem is to calculate further solutions, (x_1, λ_1), (x_2, λ_2), $\cdots$ until we reach a target point, say at $\lambda = \lambda^*$. The i^{th} continuation step starts from an approximation of (x_i, λ_i) and attempts to calculate the next solution. There is an intermediate step, however. With the predictor-corrector type continuation, the $i \rightarrow i+1$ step is split in two parts. The first predicts a solution, and the second attempts to make this prediction converge to the required solution:

Predictor $(x_i, \lambda_i) \rightarrow (\overline{x}_{i+1}, \overline{\lambda}_{i+1})$

Corrector $(\overline{x}_{i+1}, \overline{\lambda}_{i+1}) \rightarrow (x_{i+1}, \lambda_{i+1})$

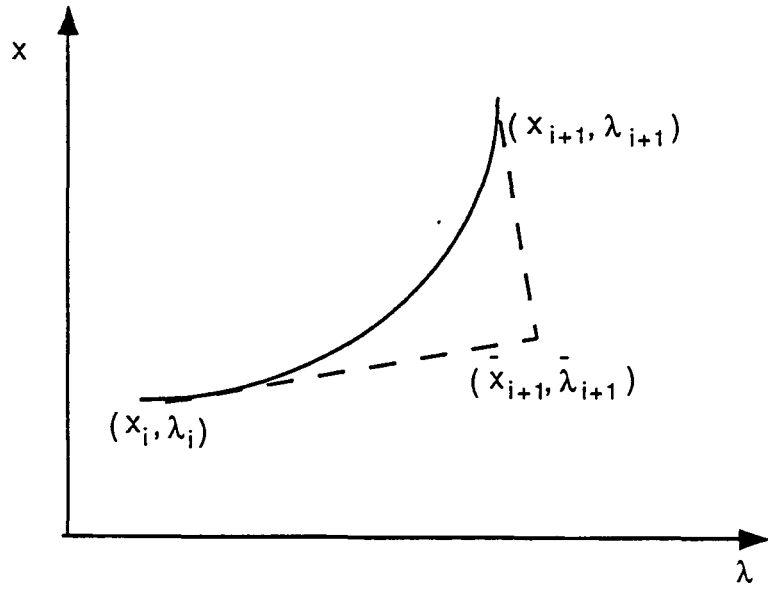

Figure 2.1: Illustration of predictor-corrector scheme

These steps are shown in Figure 2.1. Continuation methods differ, among other things, in the

1. choice of the predictor,
2. type of the parameterization strategy,
3. type of the corrector method, and
4. the step length control.

These four aspects will be explained through the formulation of the power flow equations in chapter (3), in which the basic continuation power flow will be explained. The continuation technique used, is explained with a simple example in Appendix A.

CHAPTER 3. PRINCIPLES OF CONTINUATION POWER FLOW

3.1 Introduction

As mentioned in the previous chapter, the continuation method is a mathematical path-following methodology used to solve systems of nonlinear equations. Using the continuation method, we can track a solution branch around the turning point without difficulty. This makes the continuation method quite attractive in approximations of the critical point in a power system. The continuation power flow developed at Iowa State University [8] captures this path-following feature by means of a predictor-corrector scheme that adopts locally parameterized continuation techniques to trace the power flow solution paths. The next sections explain the principles of continuation power flow.

3.2 Locally Parameterized Continuation

A parameterization is a mathematical means of identifying each solution on the branch, a kind of measure along the branch. When we say "branch," we refer to a curve consisting of points joined together in $(n+1)$ dimensional space that are solutions of the nonlinear equations

$$\mathbf{F}(\mathbf{x}, \lambda) = 0 \tag{3.1}$$

This equation is obtained by introducing a load parameter, λ, into the original system of nonlinear equations, $\mathbf{F}(\mathbf{x}) = \mathbf{0}$. For a range of values of λ, it is quite possible to identify each solution on the branch in a mathematical way [12]. But not every branch can be parameterized by an arbitrary parameter. The solution of equation 3.1 along a given path can be found for each value of λ, although problems arise when a solution does not exist for some maximum possible λ value. At this point, one of the state variables, x_i, can be used effectively as the parameter to be varied, choice of which is determined locally at each continuation step. Thus, the method is designated as the locally parameterized continuation. In summary, local parameterization allows not only the added load parameter λ, but also the state variables to be used as continuation parameters.

3.3 Formulation of Power Flow Equations

To apply locally parameterized continuation techniques to the power flow problem, the power flow equations must be reformulated to include a load parameter, λ. This reformulation can be accomplished by expressing the load and the generation at a bus as a function of the load parameter, λ. Thus, the general forms of the new equations for each bus i are

$$\Delta P_i = P_{G_i}(\lambda) - P_{L_i}(\lambda) - P_{T_i} = 0 \tag{3.2}$$

$$\Delta Q_i = Q_{G_i} - Q_{L_i}(\lambda) - Q_{T_i} = 0 \tag{3.3}$$

where

$$P_{T_i} = \sum_{j=1}^{n} V_i V_j y_{ij} cos(\delta_i - \delta_j - \gamma_{ij})$$

$$Q_{T_i} = \sum_{j=1}^{n} V_i V_j y_{ij} sin(\delta_i - \delta_j - \gamma_{ij})$$

and $0 \leq \lambda \leq \lambda_{critical}$. $\lambda = 0$ corresponds to the base case, and $\lambda = \lambda_{critical}$ to the critical case. The subscripts L, G, and T respectively denote bus load, generation, and injection. The voltage at bus i is $V_i \angle \delta_i$, and $y_{ij} \angle \gamma_{ij}$ is the $(i,j)^{th}$ element of the system admittance matrix $[y_{BUS}]$.

To simulate different load change scenarios, the P_{L_i} and Q_{L_i} terms can be modified as

$$P_{L_i}(\lambda) = P_{L_{io}} + \lambda \left[K_{L_i} S_{\Delta_{BASE}} cos(\psi_i) \right] \quad (3.4)$$

$$Q_{L_i}(\lambda) = Q_{L_{io}} + \lambda \left[K_{L_i} S_{\Delta_{BASE}} sin(\psi_i) \right] \quad (3.5)$$

where

$\mathbf{P_{L_{io}}, Q_{L_{io}}}$ = original load at bus i, active and reactive respectively;

$\mathbf{K_{L_i}}$ = multiplier designating the rate of load change at bus i as λ changes;

$\psi_\mathbf{i}$ = power factor angle of load change at bus i; and

$\mathbf{S_{\Delta BASE}}$ = apparent power, which is chosen to provide appropriate scaling of λ.

The active power generation can be modified to

$$P_{G_i}(\lambda) = P_{G_{io}}(1 + \lambda K_{G_i}) \quad (3.6)$$

where

$\mathbf{P_{G_{io}}}$ = active generation at bus i in the base case and

$\mathbf{K_{G_i}}$ = constant specifying the rate of change in generation as λ varies.

Now if F is used to denote the entire set of equations, then the problem can be expressed as a set of nonlinear algebraic equations represented by equation 3.1, with $x = [\underline{\delta}, \underline{V}]^T$. The predictor-corrector continuation process can then be applied to these equations.

3.4 The Predictor-corrector Process

The first task in the predictor process is to calculate the tangent vector. This can be obtained from

$$\left[\underline{F}_\delta, \underline{F}_v, \underline{F}_\lambda\right] \begin{bmatrix} d\underline{\delta} \\ d\underline{V} \\ d\lambda \end{bmatrix} = 0$$

On the left side of the equation is a matrix of partial derivatives multiplied by the vectors of differentials. The former is the conventional power flow Jacobian augmented by one column (F_λ), whereas the latter $t = [d\underline{\delta}, d\underline{V}, d\lambda]^T$ is the tangent vector being sought. Normalization must be imposed to give $\underline{t}$ a nonzero length. One can use, for example,

$$e_k^T \underline{t} = t_k = 1$$

where e_k is an appropriately dimensioned row vector with all elements equal to zero except the k^{th}, which is equal to one. If the index k is chosen properly, letting $t_k = \pm 1.0$ impose a nonzero norm on the tangent vector and guarantees that the augmented Jacobian will be nonsingular at the point of maximum possible system load [20]. Thus, the tangent vector is determined as the solution of the linear system

$$\begin{bmatrix} \underline{F}_\delta & \underline{F}_v & \underline{F}_\lambda \\ & e_k & \end{bmatrix} [\underline{t}] = \begin{bmatrix} 0 \\ \pm 1 \end{bmatrix} \tag{3.7}$$

Once the tangent vector has been found by solving equation 3.7, the prediction can be made as:

$$\begin{bmatrix} \underline{\delta^*} \\ \underline{V^*} \\ \lambda^* \end{bmatrix} = \begin{bmatrix} \underline{\delta} \\ \underline{V} \\ \lambda \end{bmatrix} + \sigma \begin{bmatrix} d\underline{\delta} \\ d\underline{V} \\ d\lambda \end{bmatrix}$$

where $'*'$ denotes the predicted solution, and σ is a scalar designating step size.

After the prediction is made, the next step is to correct the predicted solution. As mentioned, the technique used here is local parameterization, whereby the original set of equations is augmented by one equation specifying the value of one of the state variables. In equation form, this relation is expressed as

$$\begin{bmatrix} F(\underline{x}) \\ x_k - \eta \end{bmatrix} = 0, \qquad \underline{x} = \begin{bmatrix} \underline{\delta} \\ \underline{V} \\ \lambda \end{bmatrix}$$

where η is an appropriate value for the k^{th} element of $\underline{x}$. Once a suitable index k and the value of η are specified, a slightly modified N-R power flow method (altered only by one additional equation and one additional state variable) can be used to solve the set of equations. This procedure provides the corrector needed to modify the predicted solution found in the previous section.

3.4.1 Selecting the continuation parameter

The best method of selecting the correct continuation parameter at each step is to select the state variable with the largest tangent vector component. In short, we select the state variable evidencing the maximum rate of change near a given solution. To begin with, λ is a good choice, and subsequent continuation parameters

can be evaluated as

$$x_k : |t_k| = max\{|t_1|, |t_2|, \cdots, |t_m|\} \tag{3.8}$$

Here, $\underline{t}$ is the tangent vector. After the continuation parameter is selected, the proper value of either +1 or -1 should be assigned to t_k in the tangent vector calculation.

3.4.2 Identifying the critical point

Arriving at the stopping criterion for the continuation power flow, we we must determine whether the critical point has been reached. This can be done easily because the critical point is the point at which maximum loading (and hence maximum λ) occurs before decreasing. For this reason, at the critical point, the tangent vector component corresponding to λ (which is $d\lambda$) is zero and becomes negative once it passes the critical point. Thus, the sign of the $d\lambda$ component tells us whether the critical point has been passed or not.

The previous paragraphs summarize the basic continuation power flow. More details can be found in [21]. The basic CPF is based on a constant power load model.

3.5 Example

The basic continuation power flow previously explained is demonstrated using the a New England 30-bus test system, whose single line diagram is given in Figure 3.1. There are a total of 9 generators and 20 PQ buses in the system. Figures 3.2 and 3.3 illustrate the variation of P_{gen} and Q_{gen} with the system load (and thus λ). When λ is increased, so is the system load. This increase is shared among the system's nine generators, according to their initial generation ratio. No P_{gen} limits are considered here, as evident from the linear shape of each curve in Figure 3.2.

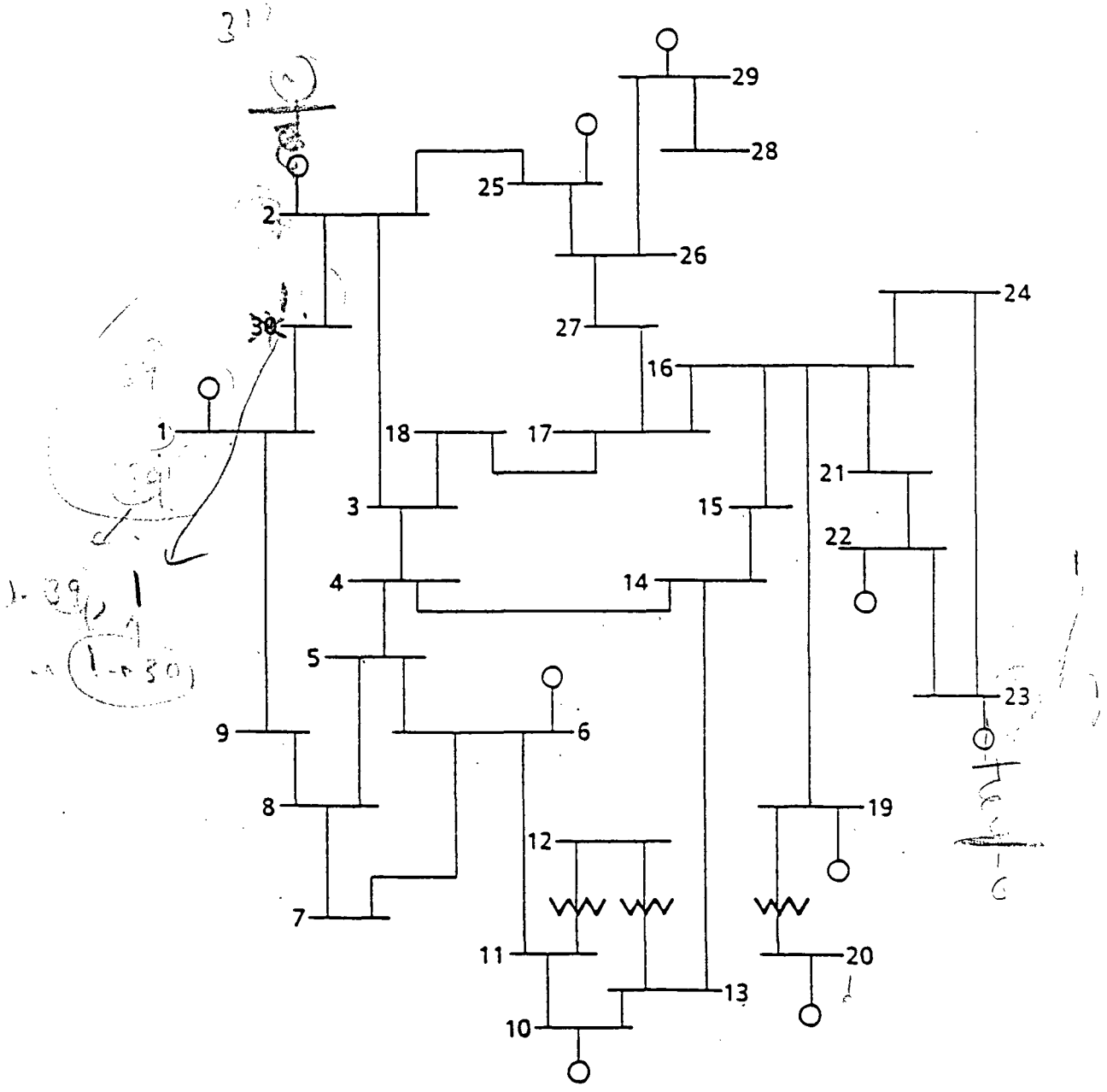

Figure 3.1: The New England 30-bus system [24]

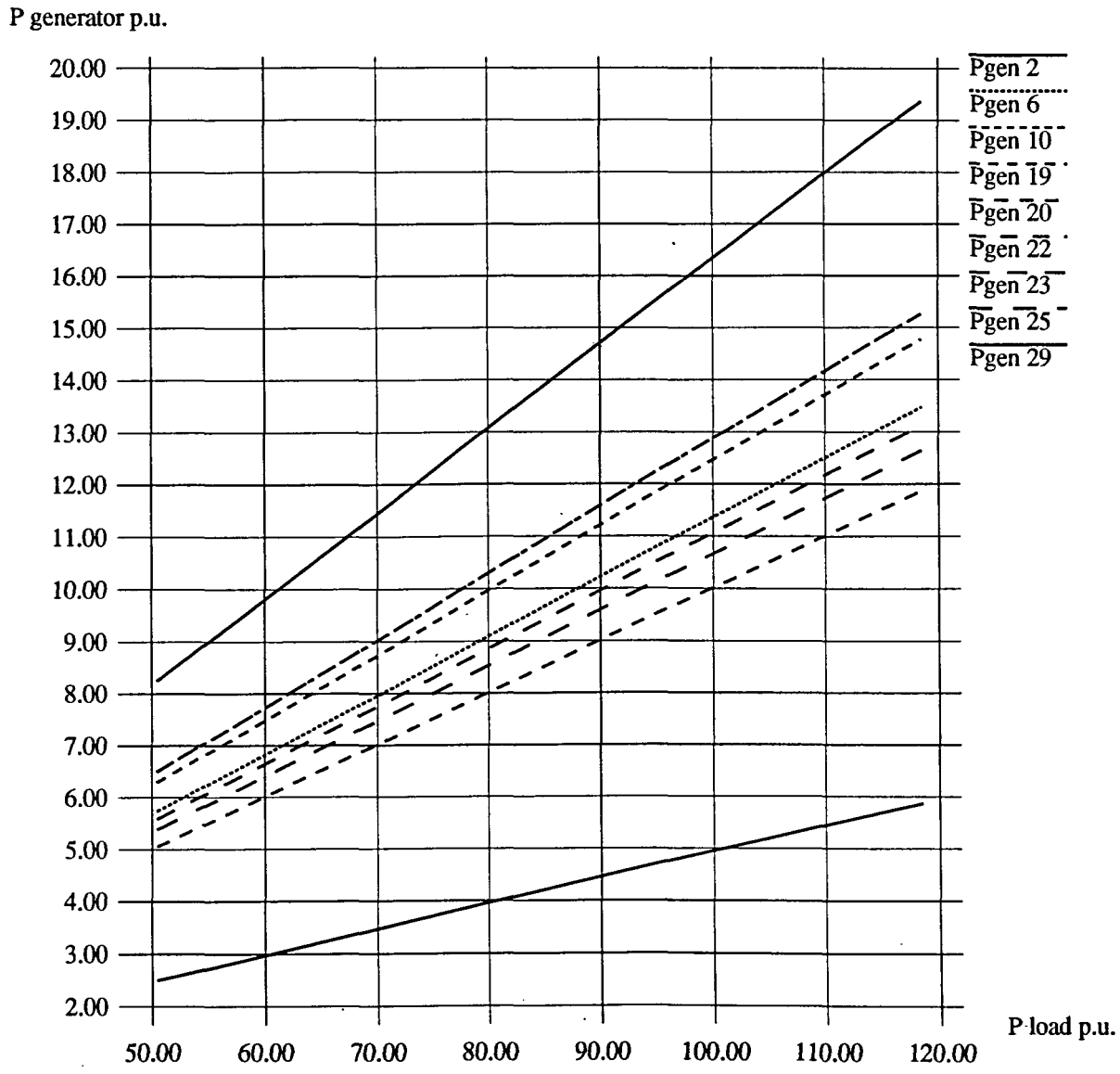

Figure 3.2: P_{gen} versus total active load curves

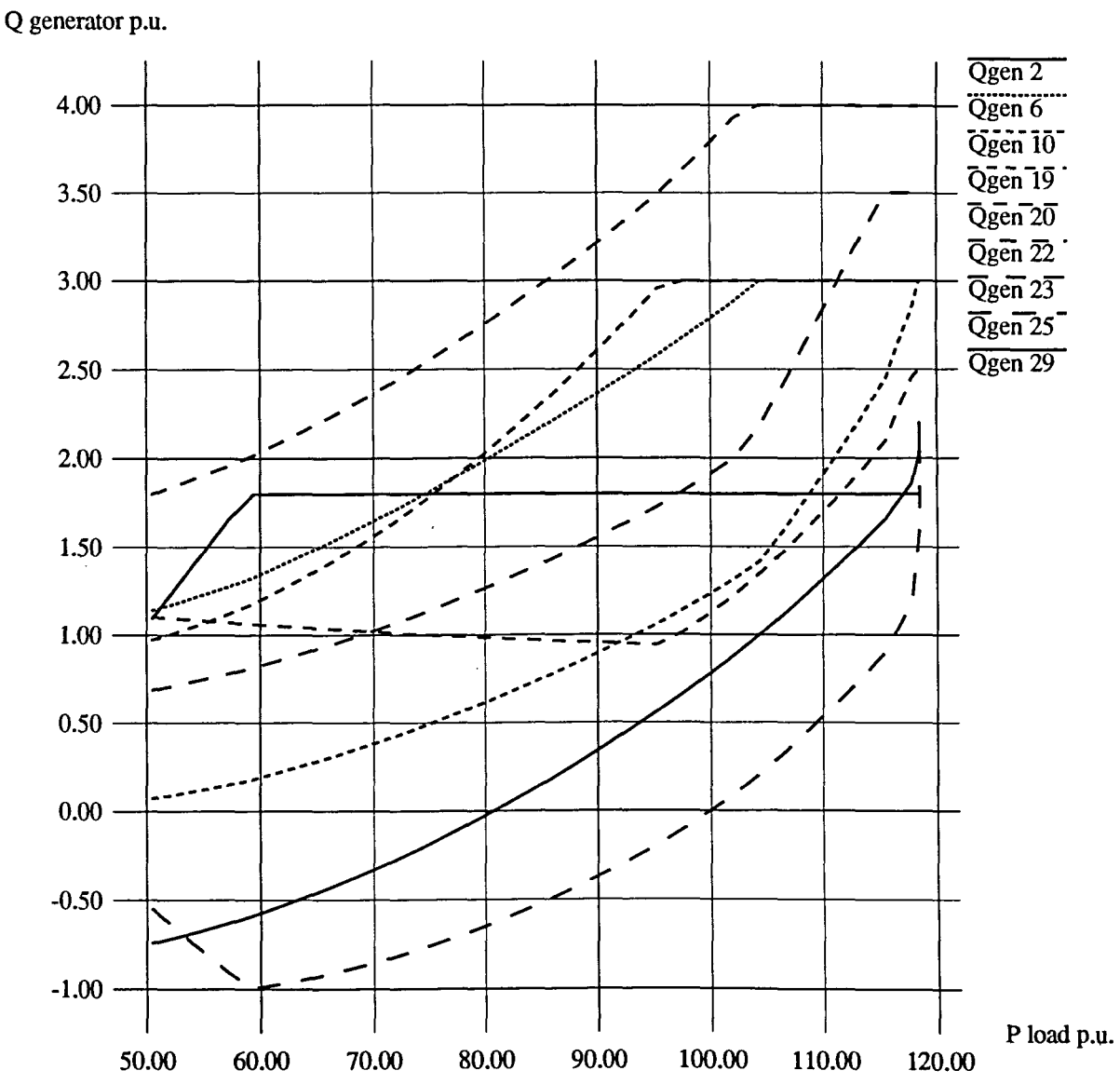

Figure 3.3: Q_{gen} versus total active load curves

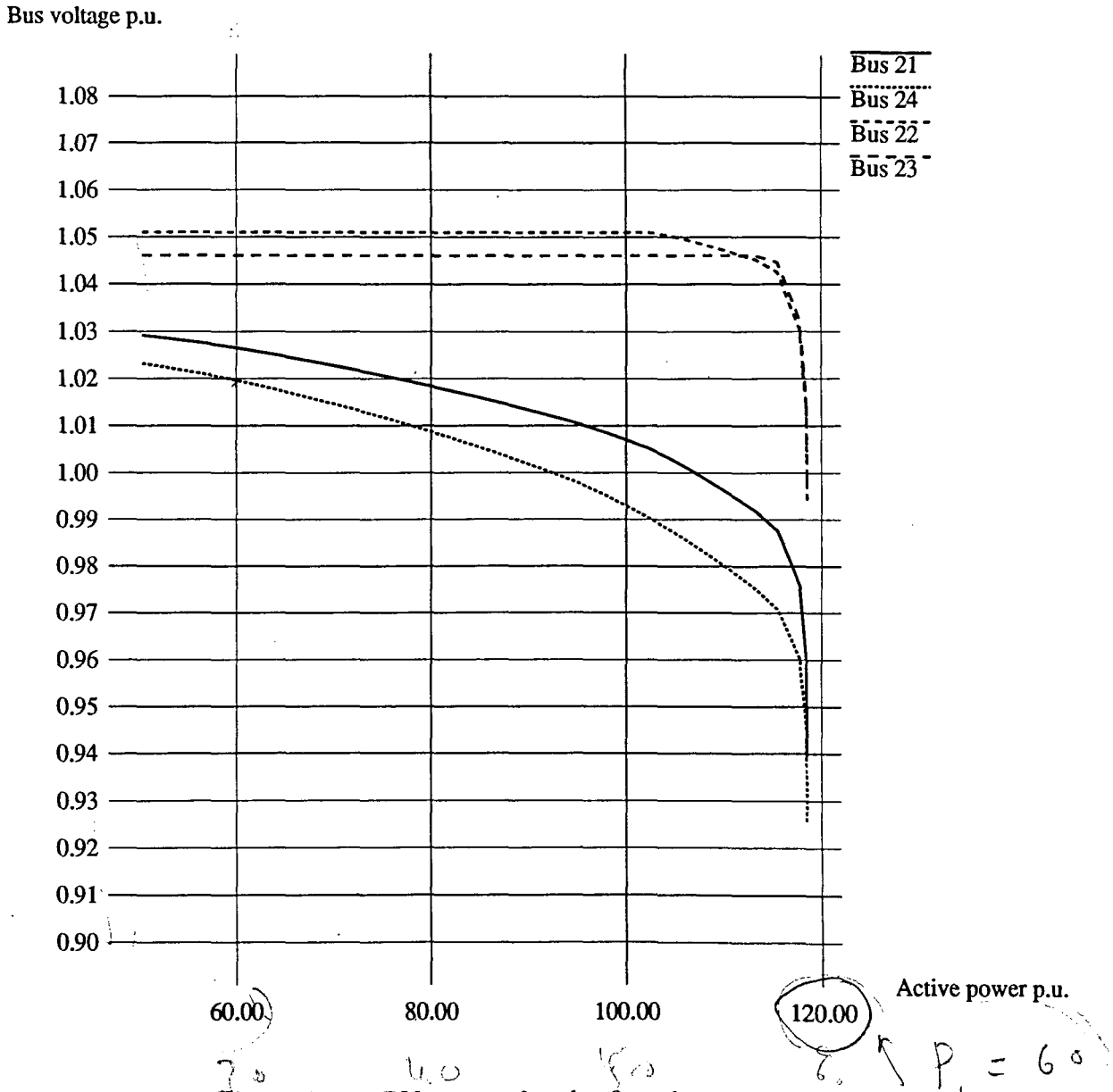

Figure 3.4: PV curves for the first four critical buses

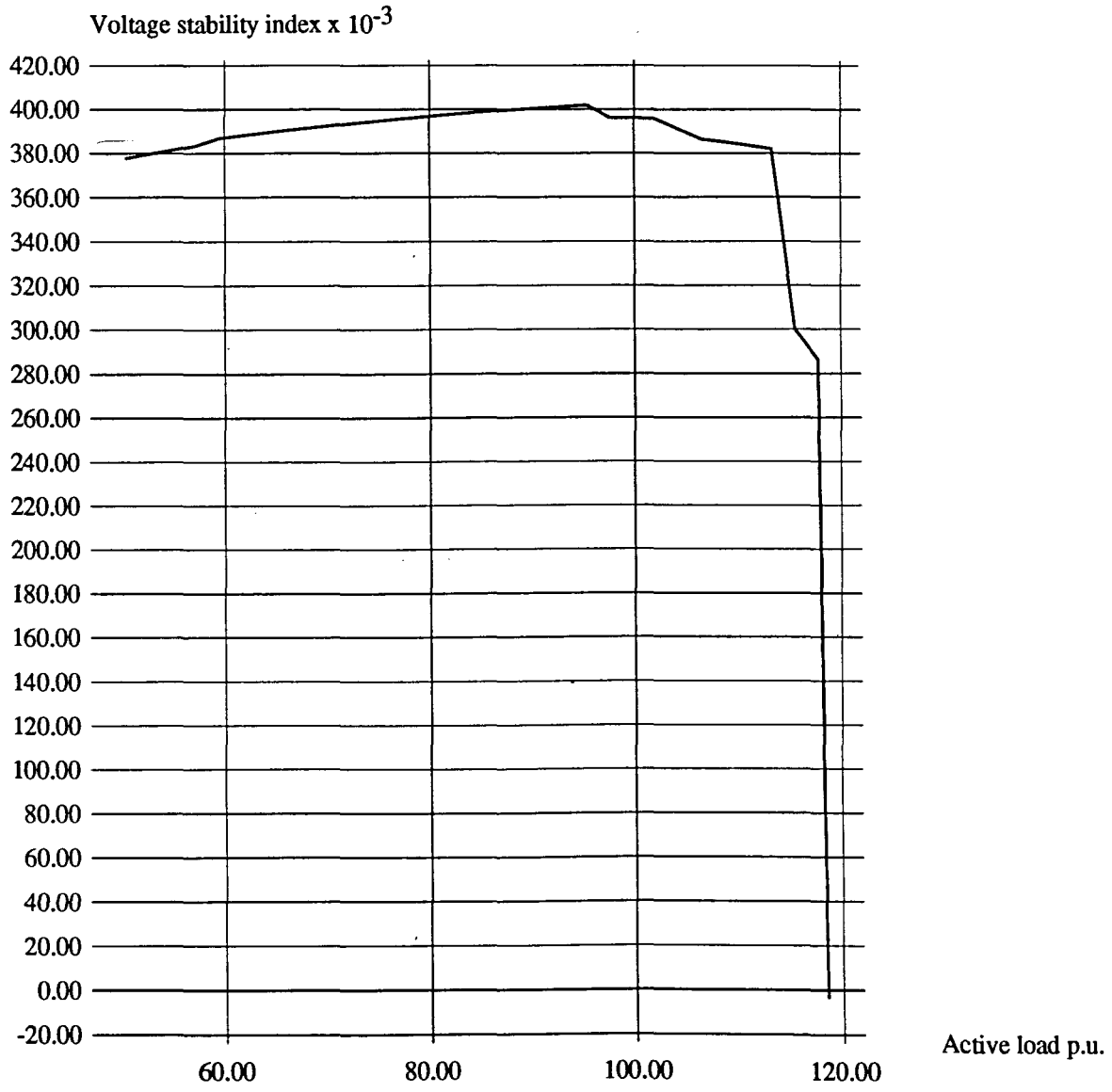

Figure 3.5: Voltage stability index trajectory for the 30-bus system

Figure 3.3 shows Q_{gen} versus total load on the system. Before the critical point is reached, seven of nine generators reach their Q_{limits}. This fact can be observed from Figure 3.3 in which the slope of a curve becomes zero once a generator reaches its Q_{limit}.

Figure 3.4 presents PV curves for the first four critical buses in the system, and Figure 3.5 gives the trajectory of the voltage stability index. Details of the critical bus selection and the voltage stability index calculations are given in Chapter 5. The index becoming zero corresponds to the system reaching the critical point. The sudden drop in the index at a certain load levels correspond to one or more units, reaching their reactive power output limits. The next chapter describes the importance of nonlinear load modeling in power systems (especially in voltage stability studies) and how these nonlinear load models are studied with CPF.

CHAPTER 4. CPF WITH NONLINEAR LOAD MODELS

4.1 Importance of Load Modeling in Power Systems

Most mathematical load models now used in power flow and transient stability studies do not represent actual load characteristics. Analysts select load models that will minimize the modeling effort. Expedience also plays a role in model selection. Thus, load models tend to yield conservative results. But the uncertainties in load modeling can be critical unknowns in the calculation of power transfer limits and in the requirements for transmission system expansion. Better models can predict power system behavior more accurately and, thus, bring improvements in transmission system planning and utilization. All told, load modeling plays an important role in the analysis of power systems.

With the objective of making more accurate, yet simple and more realistic load models based on available data, General Electric Company under the contract with EPRI [22] developed a quite sophisticated software, called load model synthesis (LOADSYN). This software is capable of producing load models for power flow and for transient stability computer studies. Actually, voltage stability studies (and hence power flow studies) often require more careful and accurate load modeling than do transient stability studies. This is because steady-state behavior changes with respect to load models, as will be demonstrated in later sections of this chapter. Here,

we are not attempting to model the loads in a power system. Rather, we are using already existing load models [22]. In this research, only the load modeling for power flow studies is considered, since we are interested only in the analysis of steady-state voltage stability.

4.2 Load Modeling in Power Flow Studies

Power flow studies are used to provide information on steady-state voltages and power flows in a system, subject to the voltage regulating capabilities of equipment and specified interchange between individual areas. The loads determine the pattern of flows and voltages within the system and should be modeled as accurately as possible. The load at any bus is a composite of many factors, including lighting, resistance heating, dc converters, arc furnaces, and motors of various sizes and types. Sensitivity of the active and the reactive loads to changes in voltage will have a significant effect on power flow results. Most power flow programs currently in use have no provisions for representing a general load dependency on voltage, since the general load is represented as constant MVA. This representation is appropriate for baseline planning studies and for steady-state evaluations following contingencies, when voltage regulating devices returned the voltage at the load to near its normal value. But for studies of voltages and flows immediately after contingencies, the representation of load's dependency upon voltage is necessary. With this in mind, we represent the load at a bus in a power flow study as a quadratic function of voltage [22]:

$$P = aV^2 + bV + c \tag{4.1}$$

where aV^2 is the constant impedance load, bV the constant current load and c the constant power load. Composition of the load at a particular bus determines the parameters a, b, and c. A similar formulation can be used for reactive power, Q. Typically, load representations in power flow programs are limited to a load-voltage relation. Load-frequency characteristics are neglected because system frequency is generally maintained within narrow limits, normally ± 0.03 Hz.

4.3 Load Models

The load on a bus consists of several types of loads such as motors, arc furnaces, and lighting. Active and reactive power requirements at a particular bus as a function of voltage depend on the types of electrical loads connected to that bus, as well as on the proportion of each type. If the quadratic load model in equation 4.1 is used, then individual loads can be represented by three analytical load models based on the load-voltage relation:

1. constant power (P = constant),
2. constant impedance ($P \propto V^2$), and
3. constant current ($P \propto V^{1.0}$).

Furthermore, a composite load may consist of any number of induction motors, synchronous motors, rectifiers, and impedance loads. For such a composite load, the load-voltage characteristic can be determined analytically by combining the effects of the above mentioned individual load models. The characteristics of each load model are described briefly here.

4.3.1 Constant power load model

$$P = VI = constant$$

This model is also referred to as constant MVA. Real and reactive power, are separately treated. To maintain constant power, the load that is modeled as constant power draws more current from the system under low-voltage conditions, and less current under high-voltage conditions. Constant power characteristics are usually valid in a limited range of supply voltages.

4.3.2 Constant impedance load model

$$P \propto V^2$$

With a constant impedance load, the both active and reactive powers increase as the square of the voltage magnitude. The active power decreases with increasing frequency. Thus, a constant impedance load absorbs much less power (both active and reactive) than a constant power load at lower voltage than at normal voltage. Consequently, the electrical load in the lines and the voltage drop at the bus during low-voltage conditions or during a fault will be different.

4.3.3 Constant current load model

$$P \propto V^{1.0}$$

The constant current load draws a constant current from the system under all voltage conditions, i.e., the power (MVA) consumed by a constant current load is directly proportional to the supply voltage. Thus, a constant current load will consume

more power (MVA) during high voltage conditions and less power (MVA) during low voltage conditions than a constant power (MVA) load. For realistic loads, a constant current load characteristic is not valid over the whole spectrum of voltages. The constant current model is nearly equivalent to 50% constant power load combined with 50% constant impedance load.

Any combination of these three types of load models yields a relatively realistic power system load model, which can be called "composite load." Developing a non-linear load model is not an easy task because system load characteristics are least known part of a power system, voltage & frequency response of the load is not well known, and data can not be easily gathered.

4.4 Continuation Power Flow for Nonlinear Loads Based on LOADSYN

The continuation power flow explained in Chapter 3 is based on a constant power load model. As mentioned, in constant power load model, load and generation at each bus are independent of voltage. Thus, both are made to vary in direct proportion to any change in λ. But in a nonlinear load model, the response of the load to a change in voltage magnitude must be considered. Developing such a model is difficult, however, inasmuch as the characteristics of a wide variety of motors, appliances, must be considered. Composition of each load class at each bus also should be estimated.

The LOADSYN software package mentioned earlier permits the user to develop load models for his or her system with a minimal amount of data on actual system loads (because of the lack of actual data) and with simply the mix of various classes, e.g., residential, commercial, and industrial. As the user acquires detailed information on load composition and characteristics, this information can be incorporated easily

to refine the model. Using LOADSYN to develop nonlinear load model for a given system requires three data sets [22]:

1. The load class mix data, describing the percentage contribution of each of several load classes to the total active power (P) load at the bus. This data must be specified for each bus or similar group of buses in the system.

2. The load composition data, describing the percentage contribution of each of several load components to the active power consumption of a particular load class. This data is a function of daily and seasonal cycles, local climate and weather, and other factors.

3. The load characteristics data, describing the electrical characteristics, e.g., power factor, voltage and frequency sensitivity and motor model parameters, of each of the load components.

Because the characteristic and composition data should not vary widely over a particular system, they can be developed once for the entire system. Only the load class mix data needs to be prepared for each bus or area and updated for changes in system load. The resultant load model is

$$P_{L_i} = P_{L_{io}} P_{a_1} (\frac{V_i}{V_{oi}})^{KPV_1} + P_{L_{io}} (1 - P_{a_1}) (\frac{V_i}{V_{oi}})^{KPV_2} \tag{4.2}$$

$$Q_{L_i} = P_{L_{io}} Q_{a_1} (\frac{V_i}{V_{oi}})^{KQV_1} + (Q_{L_{io}} - P_{L_{io}} Q_{a_1}) (\frac{V_i}{V_{oi}})^{KQV_2} \tag{4.3}$$

where these definitions pertain:

$\mathbf{P_{Lio}}, \mathbf{Q_{Lio}}$ = the initial active and reactive powers consumed by the load at bus i, respectively (from the base case);

$\mathbf{V_i}$ = the voltage at bus i

$\mathbf{V_{oi}}$ = the initial voltage at bus i (from the base case);

$\mathbf{P_{a1}}$ = the frequency-dependent fraction of the active power load;

$\mathbf{KPV_1}$ = the voltage exponent for the frequency-dependent active power load;

$\mathbf{KPV_2}$ = the voltage exponent for the nonfrequency-dependent active power load;

$\mathbf{Q_{a1}}$ = the ratio of the uncompensated reactive power load to the active power load;

$\mathbf{KQV_1}$ = the voltage exponent for the uncompensated reactive power load; and

$\mathbf{KQV_2}$ = the voltage exponent for the reactive power compensation.

Note: The full model includes terms accounting for frequency deviation. Here, only voltage dependent terms are used. Details about this software can be found in [22].

To simulate any load change in the CPF using the load model given by equations 4.2 and 4.3, the P_{L_i} and Q_{L_i} terms must be modified. This can be achieved by dividing each term into two components, as shown in equations 4.4 and 4.5. The first component corresponds to the original load at bus i, and the second component represents load change resulting from the change in the load connection parameter λ.

$$P_{L_i}(\lambda) = P_{L_i}(1 + K_{L_i}\lambda) \tag{4.4}$$

$$Q_{L_i}(\lambda) = Q_{L_i}(1 + K_{L_i}\lambda) \tag{4.5}$$

where the subscript L_i is used to denote the load at bus i. Similarly, the active power generation term can be modified to be

$$P_{G_i}(\lambda) = P_{G_{io}}(1 + \lambda K_{G_i}) \tag{4.6}$$

The same approach holds for the reactive power term. The input to the LOADSYN program is load class mix data, load composition data, and load characteristic data. The output is the set of constants P_{a_1}, Q_{a_1}, KPV_1, KPV_2, KQV_1, and KQV_2. For the constant current formulation, the voltage exponents in equations 4.2 and 4.3 become 1.0. For the constant impedance formulation, they are equal to 2.0.

Unlike the constant power load formulation, where the term λ corresponds directly to the actual load in terms of MW or MVAR, λ in this formulation corresponds to the quantity of connected motors, appliances, that has a given characteristic. In this formulation, λ is referred to as a connection parameter rather than as a load parameter. The concept of λ as a connection parameter and analyzing PV curve in the sense of steady-state voltage stability can be illustrated with a simple two-bus example.

4.4.1 Two-bus example

Consider a single source connected to a pure resistive load through a single line of reactance 0.1. The continuation power flow program is run for this example, which is similar to that considered by Sauer et al. [23]. The increase in load is merely an increase in the number of parallel resistors. The continuation parameter λ in this example can be related to the number of resistors. The physical significance of operation varies from the open circuit case (number of resistors connected = 0) to the short circuit case (number of resistors connected = ∞). Figures 4.2 and 4.3 presents λ versus P and P versus V plots for this example. Conventionally, the lower portion of the PV curve (that portion below the tip of the curve) is referred to as voltage instability. But this example shows that it is not true. Figure 4.3 demonstrates that

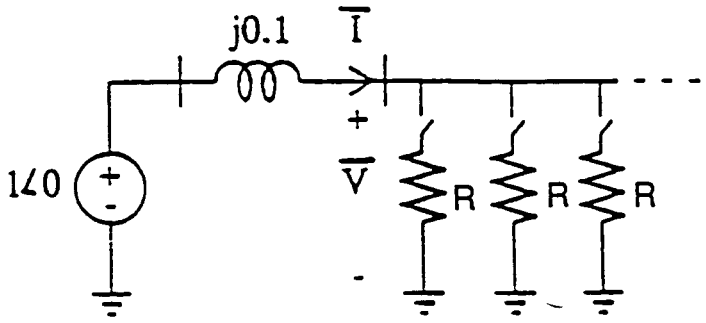

Figure 4.1: Simple two-bus example

we can operate at all points on the PV curve as long as voltage limits are satisfied. The tip of the curve (point A in the figure) is merely the maximum power transfer point and is not the critical point. The critical point is B, at which the Jacobian becomes singular. In the bifurcation literature, B is referred to as a static-fold type bifurcation. At that point, the qualitative behavior of any system changes, i.e., the system loses stability. The next section examines the results of the continuation power flow program using different load model types.

4.4.2 A test case

To demonstrate the continuation power flow with different load models, a scenario from the 30-bus New England test system was simulated. A base case load accompanying the system, as well as system data, was taken from [24]. For the composite load model, the required constants in equations 4.2 and 4.3 were obtained from

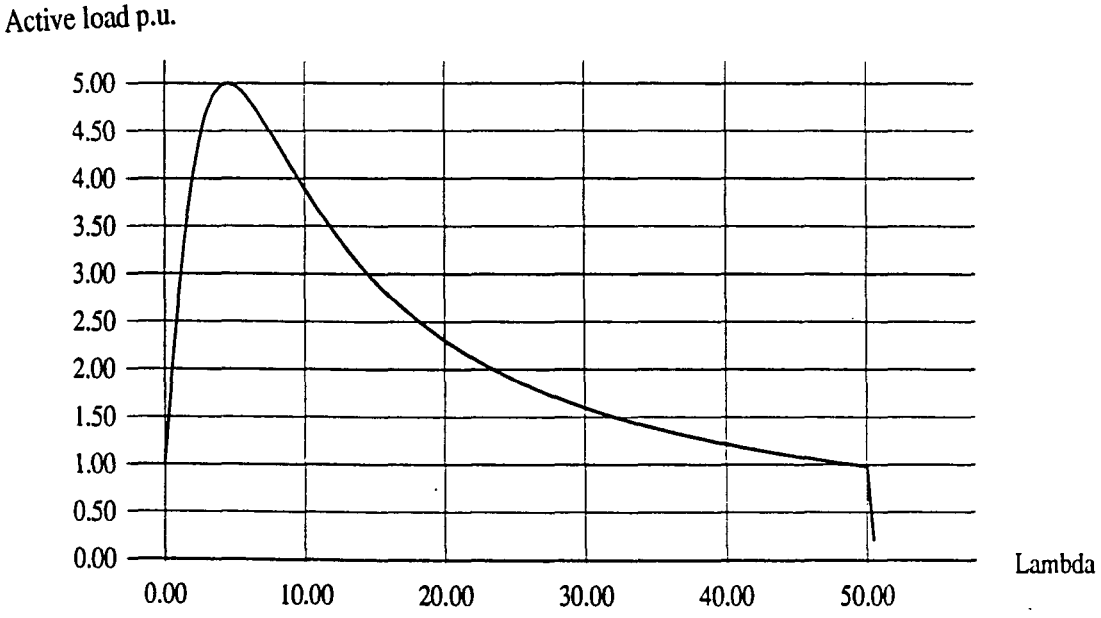

Figure 4.2: λ versus active load for 2-bus example

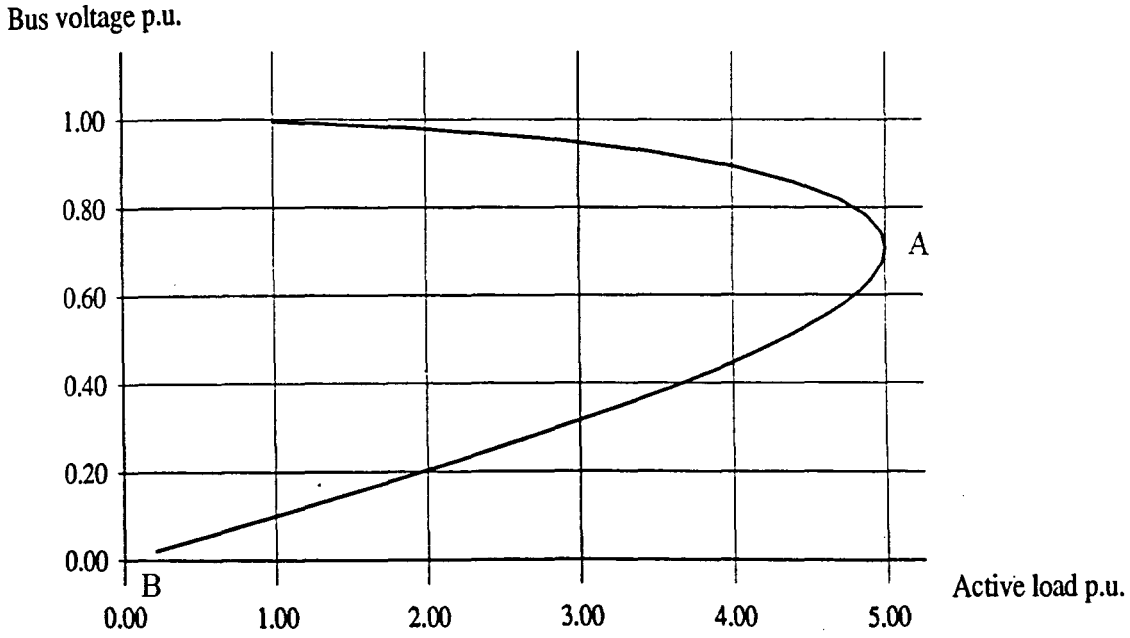

Figure 4.3: PV curve for the 2-bus example

Table 4.1: Constants used in composite load model

Constant	Value
Pa_1	0.70
KPV_1	0.38
KPV_2	1.78
Qa_1	0.44
KQV_1	1.64
KQV_2	2.00

Table 4.2: P_{max} and $P_{critical}$ values for different load models using CPF

Type of load	P_{max} (MW)	$P_{critical}$ (MW)
Constant Power	95.75	95.75
Constant Current	109.26	87.08
Constant Impedance	111.05	80.95
Composite load	110.59	98.01

the LOADSYN program. For the load class mix data, a composition of 35% heavy industrial, 35% commercial, and 30% residential load was considered. The resulting sets of constants are shown in Table 4.1 [21]. Figures 4.4-4.11 show the load variation with respect to λ and PV curves for constant power, constant current, constant impedance, and composite (based on LOADSYN) load models. As expected, with the constant power load model, the load changes linearly, for a change in λ. But for the other three types of load models, hysteresis can be seen. That is, the power reaches a maximum before a maximum in the load connection parameter λ occurs.

Table 4.2 shows the P_{max} and $P_{critical}$ values for the four types of load models. P_{max} is equal to $P_{critical}$ for constant power load model. But they are distinct (P_{max} is greater than $P_{critical}$) for the other three load models. Physically, this can be interpreted as follows: after the maximum power transfer occurs, more load is be-

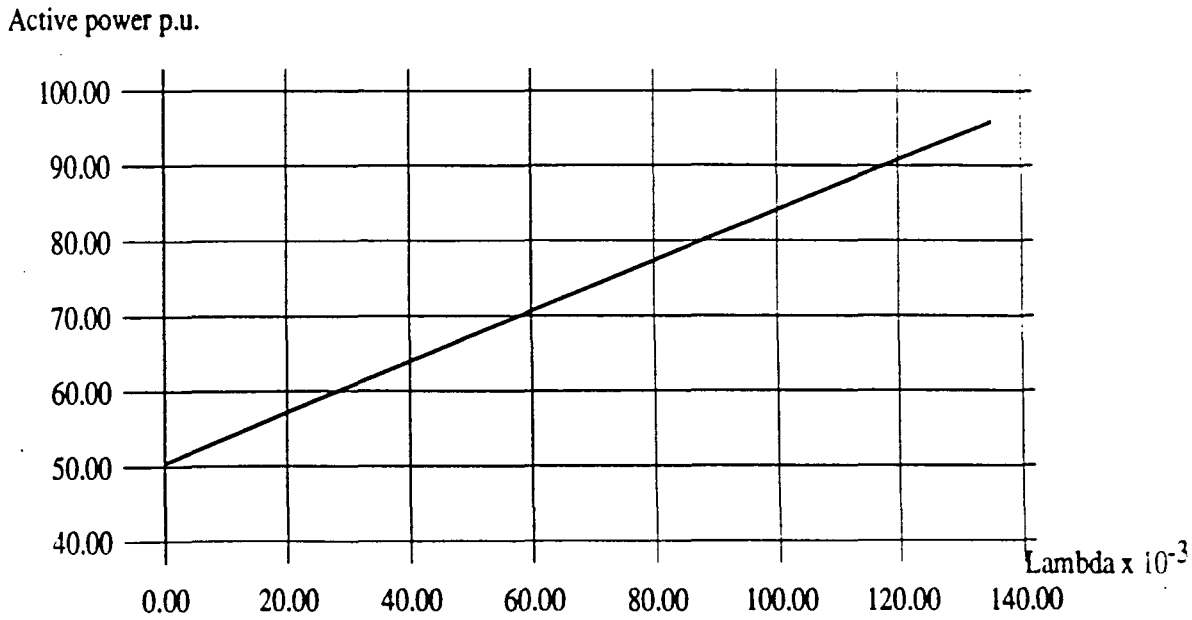

Figure 4.4: λ versus active load for the constant power load model

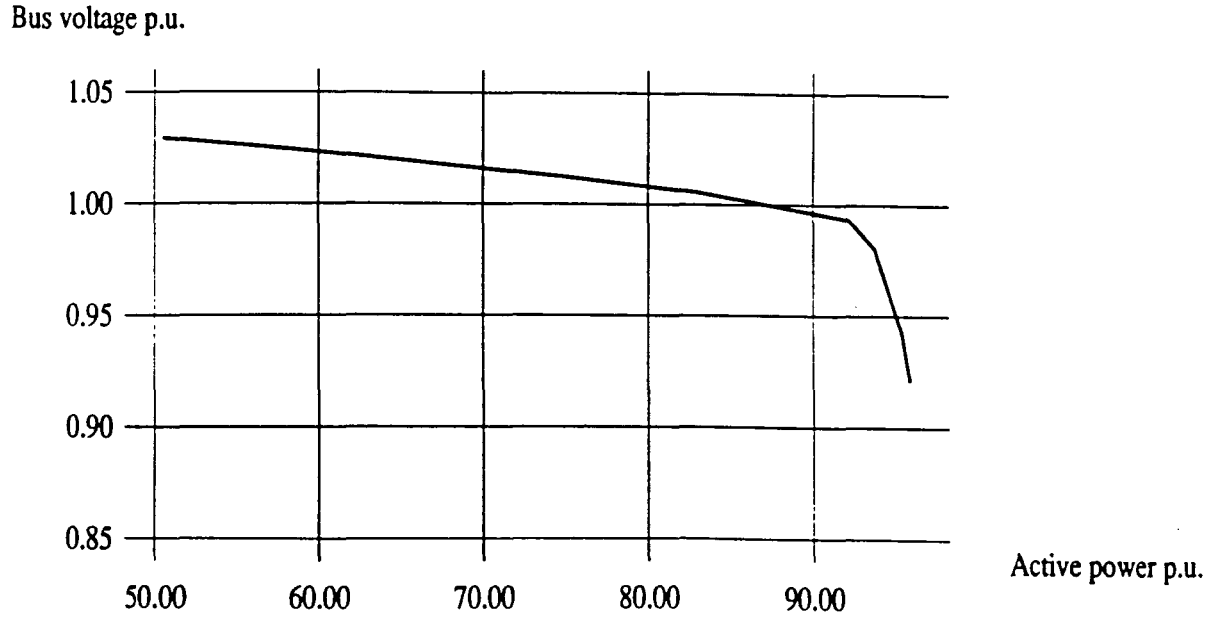

Figure 4.5: PV curve for the constant power load model

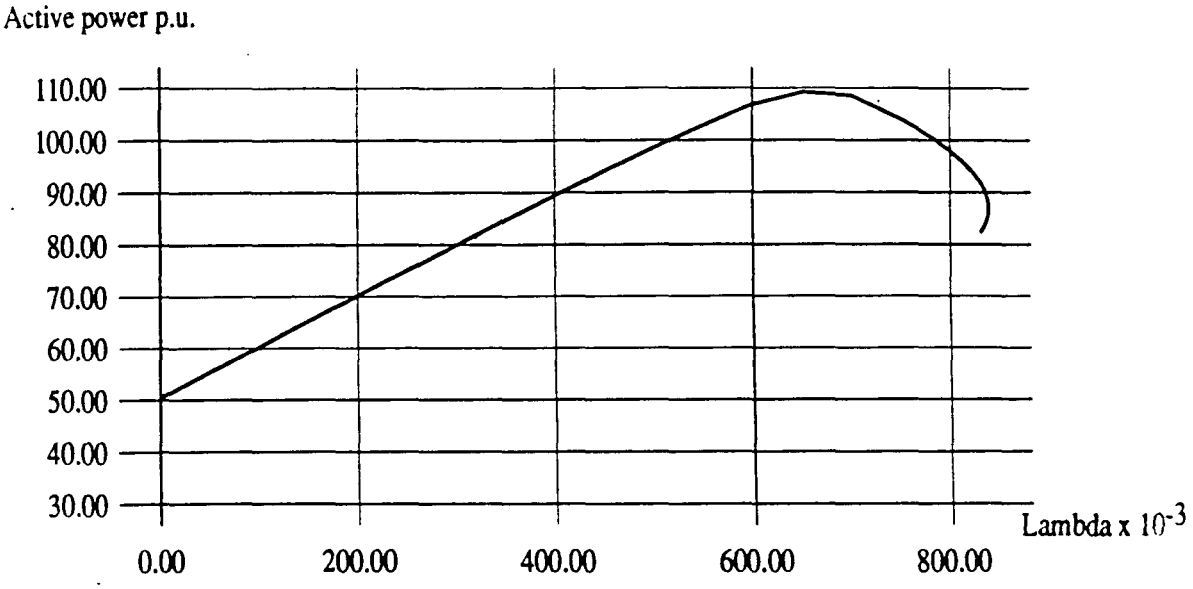

Figure 4.6: λ versus active load for the constant current load model

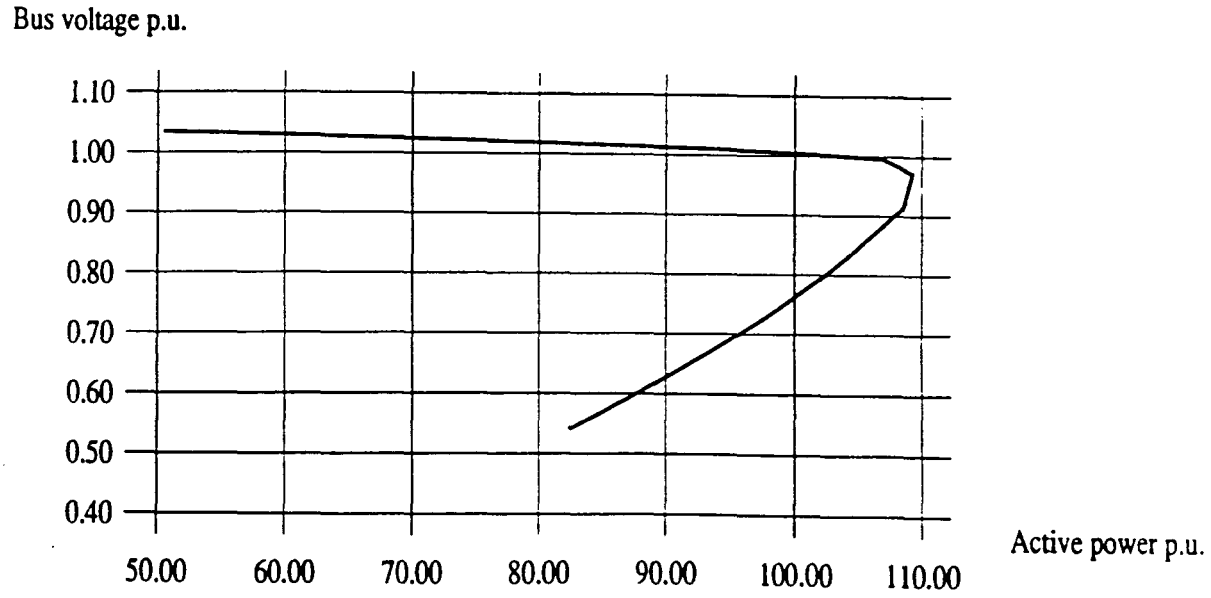

Figure 4.7: PV curve for the constant current load model

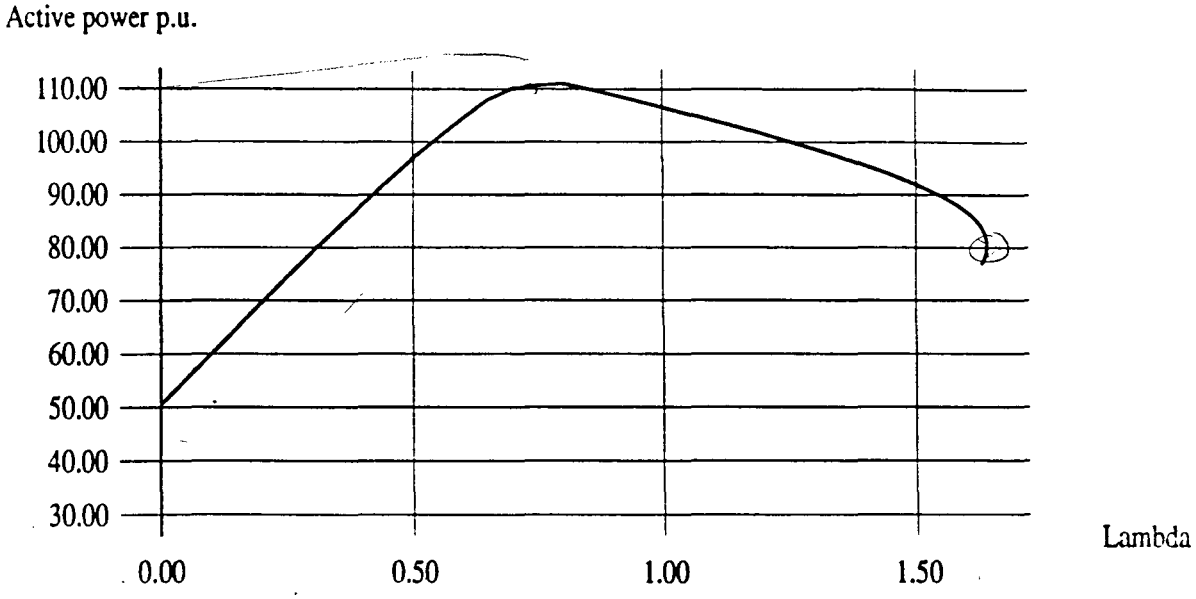

Figure 4.8: λ versus active load for the constant impedance load model

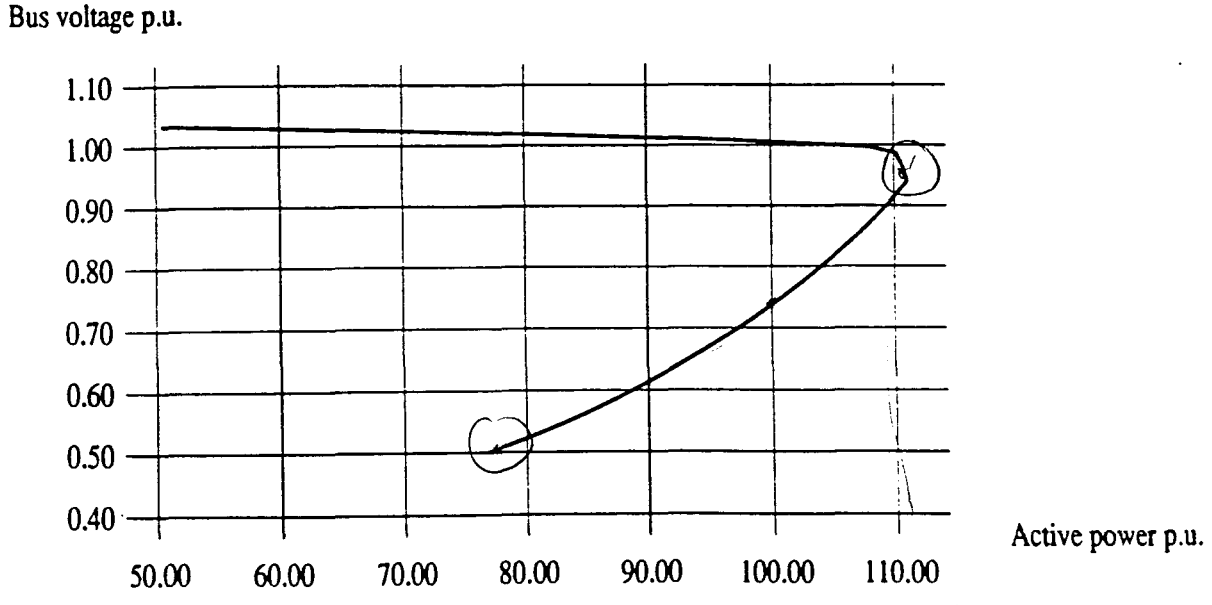

Figure 4.9: PV curve for the constant impedance load model

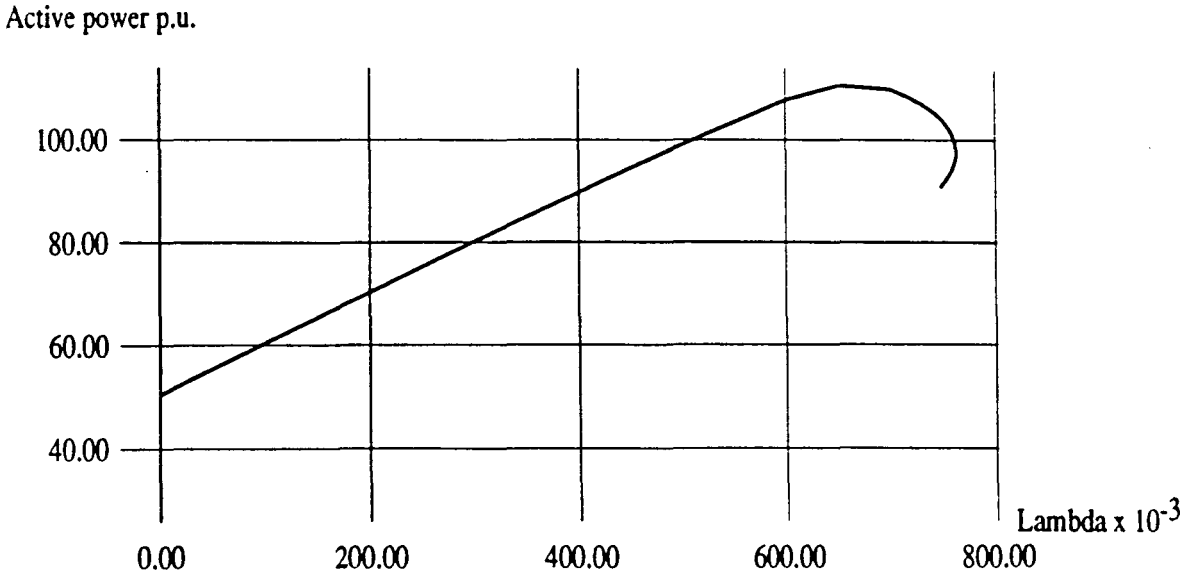

Figure 4.10: λ versus active load for the composite load model

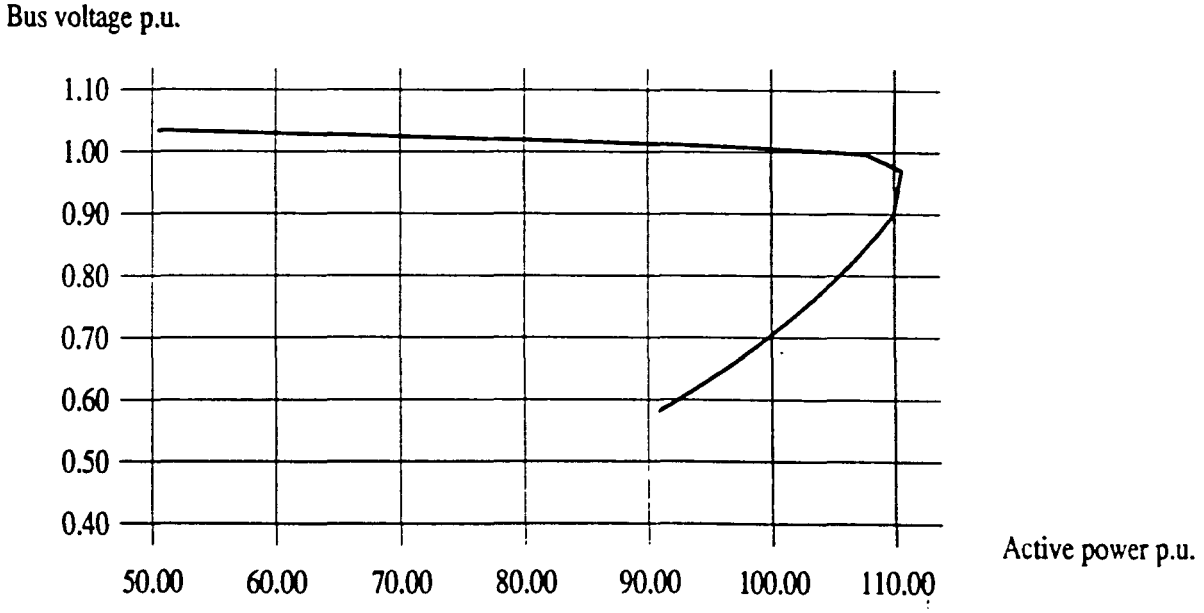

Figure 4.11: PV curve for the composite load model

ing connected, but actual power consumption decreases as a result of the dominating effect of the load voltage dependency.

The Jacobian becomes singular at the operating point corresponding to $P_{critical}$, but not at the operating point corresponding to P_{max}. These examples (2-bus and 30-bus) clarify our understanding of the critical point with respect to the PV curves. Previously, the tip of the PV curve was assumed to be the critical point. The upper portion of the curve was considered stable, and the lower portion unstable. This demonstration clearly avoids such ambiguity. Moreover, the maximum power transfer is less for the constant power load model than for the other types of load models. Thus, the constant power load model is relatively conservative.

It should be noted that although the LOADSYN software yields a better load model than the standard load models now available, there is still room for improvement. For example, the range of voltage and frequency changes over which the models are valid was not investigated thoroughly during the development of LOADSYN. Further research is needed to improve model accuracy over a wide range of voltage and frequency. In particular, further investigation of the behavior and the modeling of motors at low voltages is needed. Also, it is extremely important to note that LOADSYN speaks only to the response of the load model to changes in voltage and frequency. It does not speak to the accuracy of the load model to the actual system load. The next chapter explains the sensitivity approach we are proposing for the analysis of steady-state voltage stability.

CHAPTER 5. SENSITIVITY BASED STEADY-STATE VOLTAGE STABILITY ANALYSIS

5.1 Introduction

The aim of continuation power flow, as described in Chapter 3, is not simply to calculate the critical point closely, but also to provide sensitivity information that can be used to identify critical components in the system. This chapter describes how the tangent vector information from the continuation power flow is used to locate weak areas in the system. In particular, it identifies buses, branches, and generators that are critical to maintain voltage stability by deriving sensitivities of these elements for a given change in load connection parameter. Results of these sensitivities obtained using a 30-bus test system and a 17-generator (162 bus) reduced Iowa system are presented to illustrate the applicability of this approach. The next section outlines existing methods for calculating these sensitivities. Later sections use the tangent vector to describe our sensitivity approach.

5.2 Identification of Critical Elements

Identifying critical elements involves locating the key components in a power system (buses, branches, or generators) that are critical to maintain voltage stability. In other words, one should find the weak areas in the system. Different authors present

different approaches for finding such areas. Modal analysis is one such approach.

5.2.1 Modal analysis

Proposed by Gao et al. [25], modal analysis involves calculation of eigenvalues and eigenvectors of the power flow Jacobian. With a steady-state power system model, the authors computed a specified number of eigenvalues and the corresponding eigenvectors of the (reduced) Jacobian. Assume ξ_i and η_i are, respectively the right and left eigenvectors of the Jacobian corresponding to the eigenvalue λ_i. Then the i^{th} modal reactive power variation is

$$\Delta Q_{m_i} = K_i \xi_i$$

where ${K_i}^2 \sum_{j=1}^{n} {\xi_{ji}}^2 = 1$, and the corresponding i^{th} modal voltage variation is

$$\Delta V_{m_i} = \frac{1}{\lambda_i} \Delta Q_{m_i}$$

If ΔV_{mi} is known, $\Delta \delta_{mi}$ can be calculated from the power flow equations. Different participations are defined as follows.

Bus participations: Participation of bus k to mode i is

$$P_{ki} = \xi_{ki} \eta_{ki}$$

where ξ_{ki} is the k^{th} element of the i^{th} column right eigenvector and η_{ki} is the k^{th} element of the i^{th} row left eigenvector.

Branch participations: The participation of branch lj to mode i is

$$P_{lj_i} = \frac{\Delta Q_{lj_i}}{\Delta Q_{lmax_i}}$$

where $\Delta Q_{lmax_i} = \text{Max}(\Delta Q_{lj_i})$ and ΔQ_{lj_i} is the linearized reactive loss variation across branch lj.

Generator participations: The participation of generator gk to mode i is

$$P_{gk_i} = \Delta Q_{gk_i} / \Delta Q_{gmax_i}$$

where $\Delta Q_{gmax_i} = \text{Max}(\Delta Q_{gk_i})$ and ΔQ_{gk_i} is the linearized reactive power output variation at generator gk.

In the three foregoing participations, the suffix i indicates a particular mode, i, corresponding to the eigenvalue λ_i. The greater the participation, the greater that component's contribution to that particular mode. Gao et al. used these participations to identify the buses, branches, and generators contributing to a particular mode, for both a base and a critical case.

5.2.2 Singular value decomposition

Another voltage stability assessment technique, based on the singular value decomposition of the power flow Jacobian, is presented by Tiranuchit et al. [4] and expanded upon by Löf et al. [26]. Singular value decomposition is described here:

Consider an $n \times n$ real matrix A. The singular value decomposition (SVD) of A is written [27]

$$A = QSP^T = \sum_{i=1}^{n} s_i q_i {p_i}^t$$

where S is an $n \times n$ diagonal matrix and Q and P are $n \times n$ orthonormal matrices. The diagonal elements of S are called singular values of A. The columns $q_1, q_2, \cdots, q_n$ of Q are called the right singular vectors. The columns $p_1, p_2, \cdots, p_n$ of P are

called the left singular vectors. By appropriate choice of Q and P, singular values can be arranged such that $s_1 \geq s_2 \geq \cdots \geq s_n \geq 0$.

For a real symmetric matrix A, the individual singular values are equal to the square root of the individual eigenvalues of $A^T A$ or AA^T [28]. Thus, for a real symmetric matrix, the absolute values of eigenvalues are equal to the singular values. Additionally, the smallest singular value of A is the 2-norm distance of A to the set of all rank-deficient matrices [28]. If the minimum singular value is zero ($i.e., s_n = 0$), then the matrix A is singular. Thus, in our voltage stability studies, the minimum singular value of the Jacobian becoming zero corresponds to the critical mode of the system. In [26], the authors calculated the minimum singular value and the two corresponding (left and right) singular vectors of the power flow Jacobian. They defined a voltage stability index as the minimum singular value of the power flow Jacobian, which indicates the distance between the studied operating point and the steady-state voltage stability limit. The next section explains how the same participation information corresponding to critical mode can be obtained and how a voltage stability index can be derived from the tangent vector of the continuation power flow. This approach requires neither eigenvalue and eigenvector evaluation, nor singular value decomposition.

5.3 Tangent Vector

In the continuation process described in Chapter 3, the tangent vector proves useful because it describes the direction of the solution path at a corrected solution point. A step in the tangent direction is used to estimate the next solution. But if we examine the tangent vector elements as differential changes in bus voltage angles ($d\delta_i$)

and magnitudes (dV_i) in response to a differential change in load connectivity ($d\lambda$), the potential for meaningful sensitivity analysis becomes evident. The next examples demonstrate how the tangent vector elements change for different load levels. The numerical results that are presented in this chapter are from the New England 30-bus system, which is a widely-used test system for voltage stability studies. Results from a 17-generator (162-bus) reduced Iowa system are also presented to illustrate the applicability of the approach to large-scale systems.

Figures 5.1 and 5.2 illustrate the tangent vector elements versus the element number for two cases with different load levels, i.e., base case (light load) and critical case (heavy load). It should be noted that the first half of the graphs (first 29 elements for 30-bus system, and first 161 elements for the 17-generator system) corresponds to voltage angle terms and that the next half (elements 30 to 49 for 30-bus system, and 162 to 316 for 17-generator system) corresponds to voltage magnitude terms. If we consider the first half of the graph (i.e., up to the elements which corresponds to voltage angle), the voltage angle terms are dominant for the light load condition than for the heavy load condition. Whereas the second half of the graph tells us that the voltage magnitudes are dominant for the heavy load condition than for the light load condition. We can conclude from this, that under light load conditions in the network, the steady-state angle stability is the less stable mode of instability, whereas under heavy load conditions the system is closer to steady-state voltage instability. The same conclusion was reached by Löf et al. [26] by performing singular value decomposition of the power flow Jacobian, which is computationally costly. But in continuation power flow we can derive the same conclusion from the tangent vector without the extra effort.

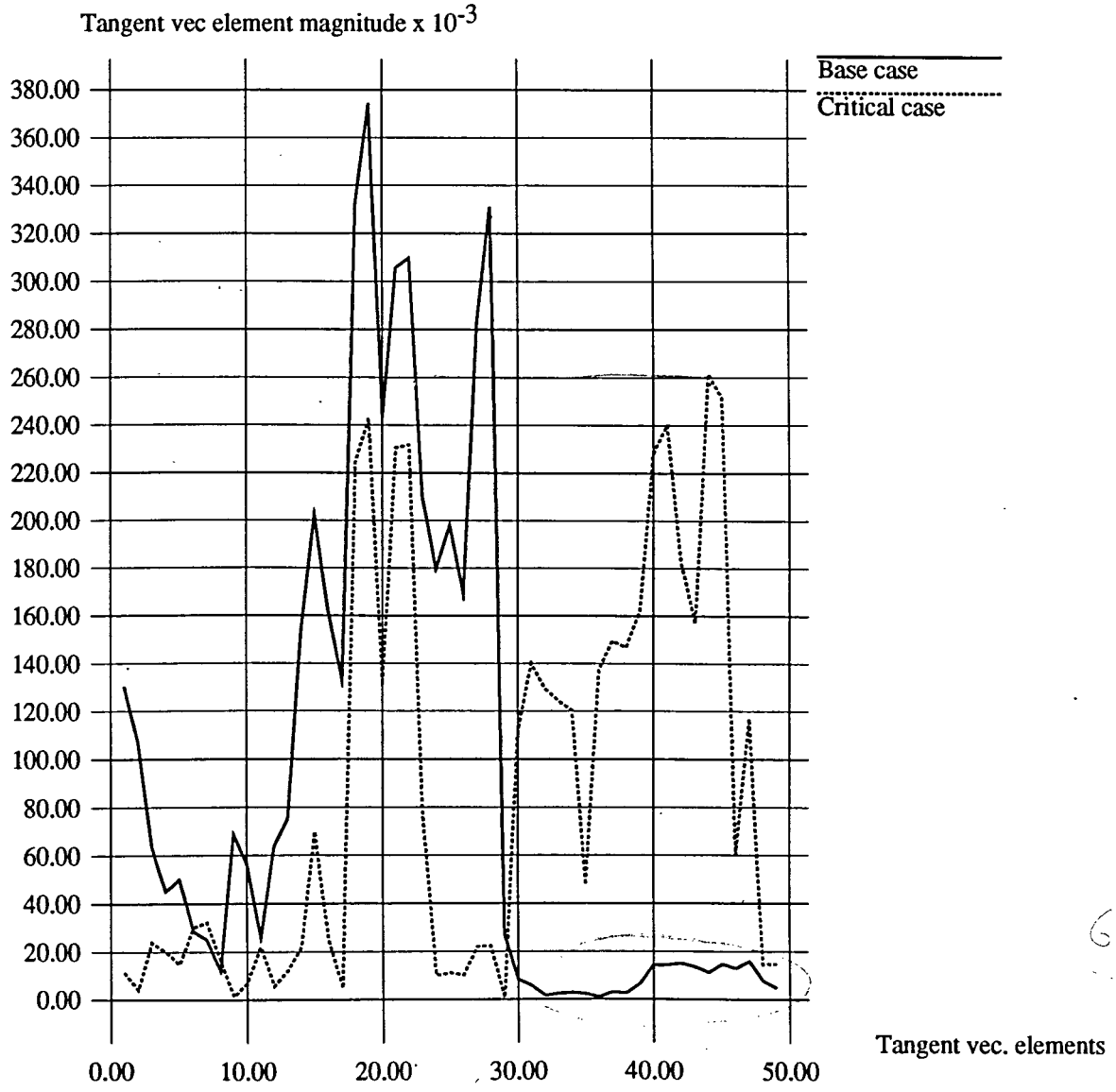

Figure 5.1: Tangent vector elements for the two cases with different load levels - 30-bus system

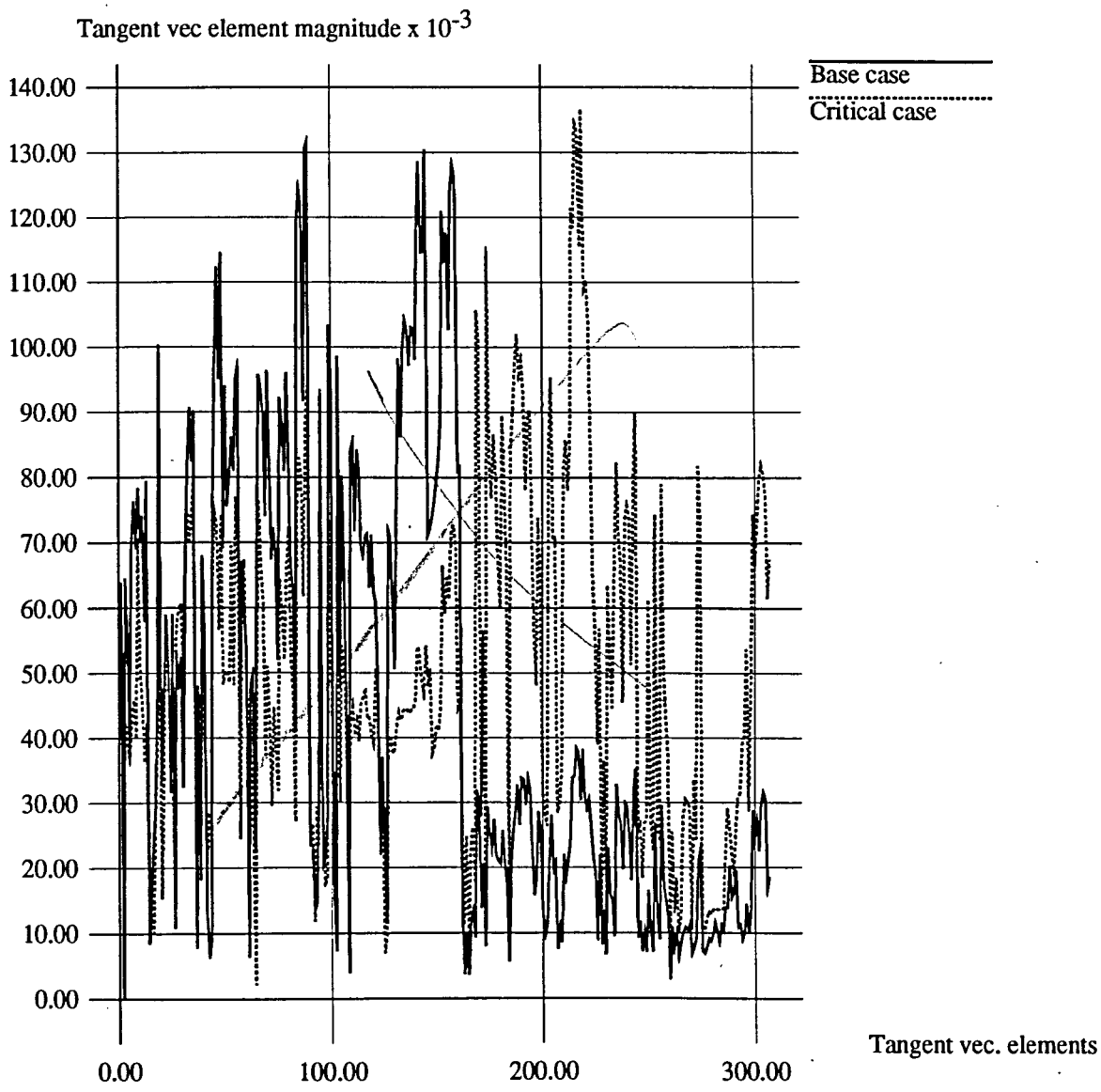

Figure 5.2: Tangent vector elements for the two cases with different load levels - 17-generator system

5.3.1 Tangent vector, right eigenvector, and right singular vector of J

Examining equation 3.7 from which the tangent vector is calculated, we can surmise that the tangent vector is the right eigenvector of the Jacobian corresponding to zero eigenvalue at the critical point. Additionally, the right eigenvector is equal to the right singular vector because the Jacobian is real and (almost) symmetric. Thus, at the critical point, the tangent vector is equal to the right eigenvector corresponding to the minimum eigenvalue and the right singular vector corresponding to the minimum singular value. This equivalence is evident from Figures 5.3 and 5.4, in which the tangent vector, the right eigenvector, and the right singular vector of the Jacobian matrix near the critical point are plotted on the same graph for both systems. This information from the tangent vector can be used to identify buses, branches, and generators that are critical to maintain voltage stability. The next section shows how a voltage stability index can be derived from the tangent vector.

5.3.2 Voltage stability index from the tangent vector

Ajjarapu et al. [8] derived a voltage stability index using tangent vector information. Their first step was to find the weakest bus with respect to voltage stability. This is same as finding the bus with the greatest dV_i/dP_{total} value. Here dP_{total} is the differential change in active load for the whole system and is given by

$$dP_{total} = \sum_n dP_{L_i} = \left[S_{\Delta_{BASE}} \sum_n K_{L_i} cos(\psi_i) \right] d\lambda = C d\lambda \qquad (5.1)$$

The weakest bus, j, is

$$|\frac{dV_j}{C d\lambda}| = max \left[|\frac{dV_1}{C d\lambda}|, |\frac{dV_2}{C d\lambda}, \cdots, |\frac{dV_n}{C d\lambda}| \right]$$

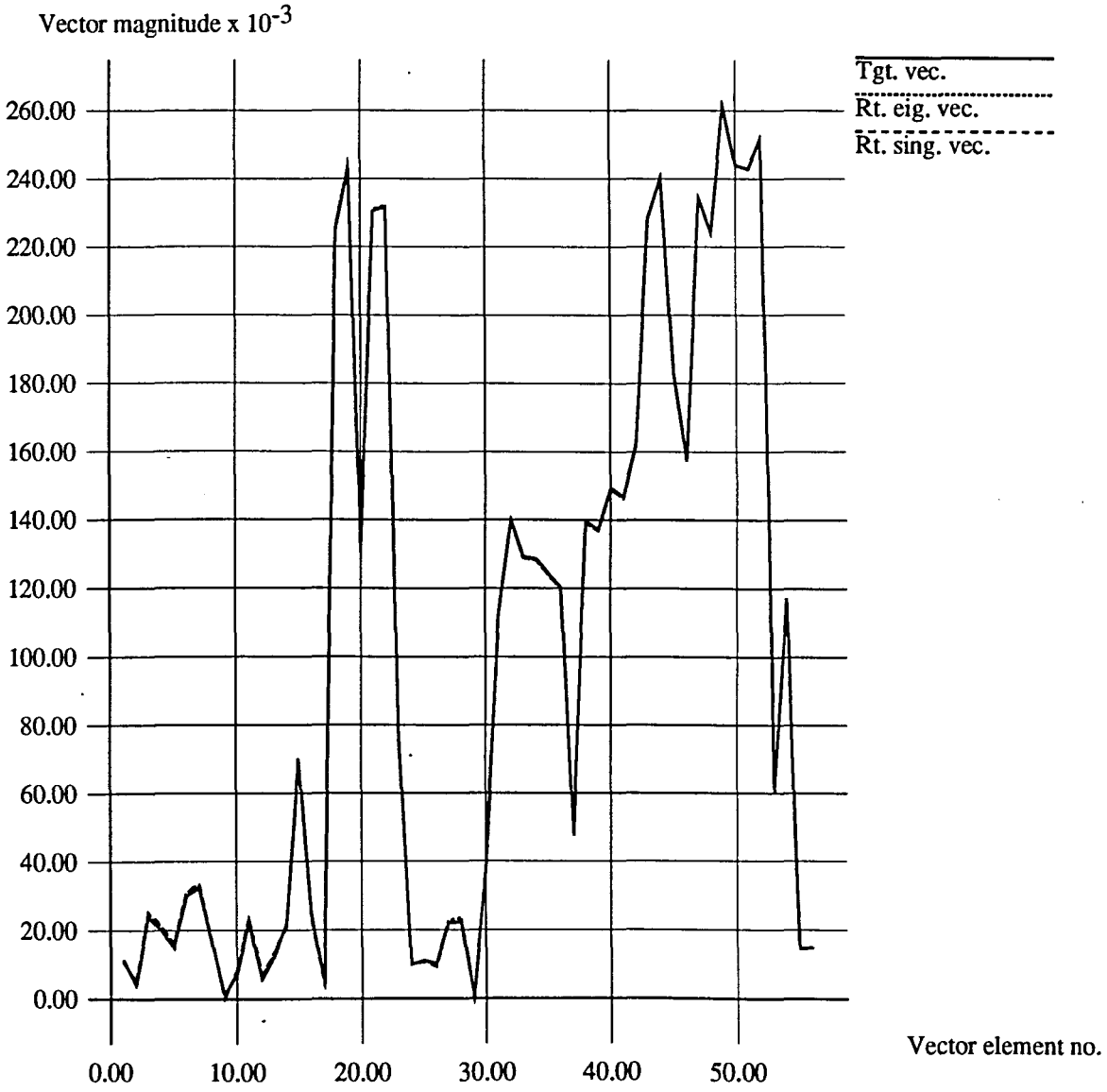

Figure 5.3: Elements of tangent vector, right eigenvector, and right singular vectors near the critical point - 30-bus system

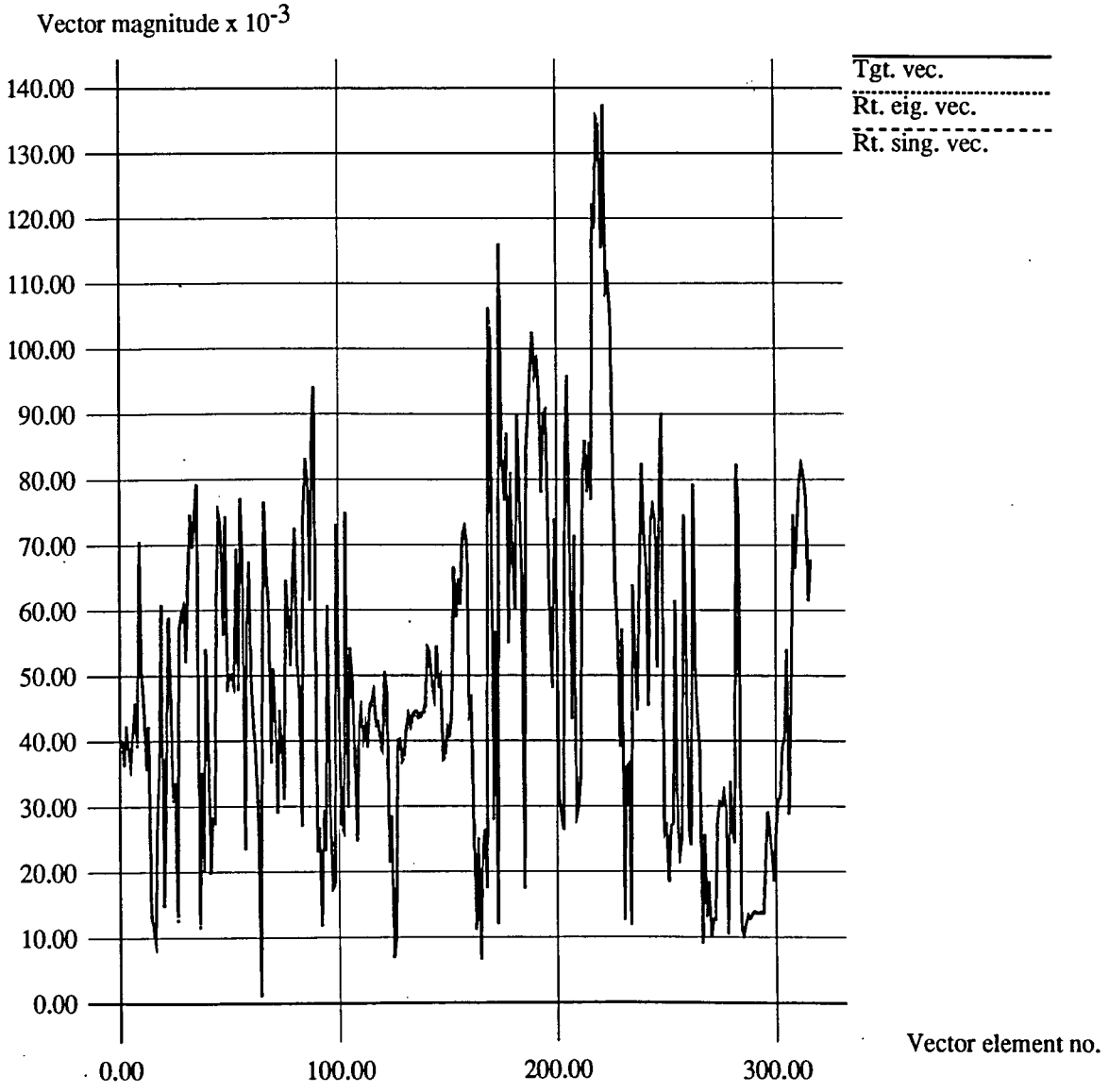

Figure 5.4: Elements of tangent vector, right eigenvector, and right singular vectors near the critical point - 17-generator system

When j reaches its steady-state voltage stability limit, $d\lambda$ approaches zero, the ratio $dV_j/Cd\lambda$ becomes infinite or equivalently the ratio $Cd\lambda/dV_j$ tends to zero. The ratio $Cd\lambda/dV_j$, which is easier to handle numerically, can be defined as a voltage stability index for the entire system. In [31] the minimum real part of the eigenvalue of the Jacobian and in [26], the minimum singular value of the Jacobian are defined as voltage stability indexes. But our tangent vector directly yields a good voltage stability index and avoids additional numerical computations. Figure 5.5 compares the voltage stability index from the tangent vector with that from the minimum eigenvalue and from the minimum singular value. The same trend is evident in the shape of the curves. All three indices are becoming zero at the same point, which indicates that the critical point has been reached. In fact, our voltage stability index has a physical interpretation in the sense that it is the ratio of differential change in voltage to differential change in active load for the whole system. The next section explains how to calculate the sensitivities of key components in the system.

5.4 Sensitivity Analysis From the Tangent Vector

In this research, we are only interested in the sensitivity of system response with respect to a change in one parameter [29]. In other words, we derive an expression for the differential change in a scalar valued function $h(x, \lambda)$, because of differential change in λ. Here, $h(x, \lambda)$ is any power system operating constraint such as branch flow, reactive output of a generator, or bus voltage magnitude. Using the differential chain rule, we obtain

$$\frac{dh}{d\lambda} = \frac{\partial h}{\partial x}\frac{dx}{d\lambda} + \frac{\partial h}{\partial \lambda} \tag{5.2}$$

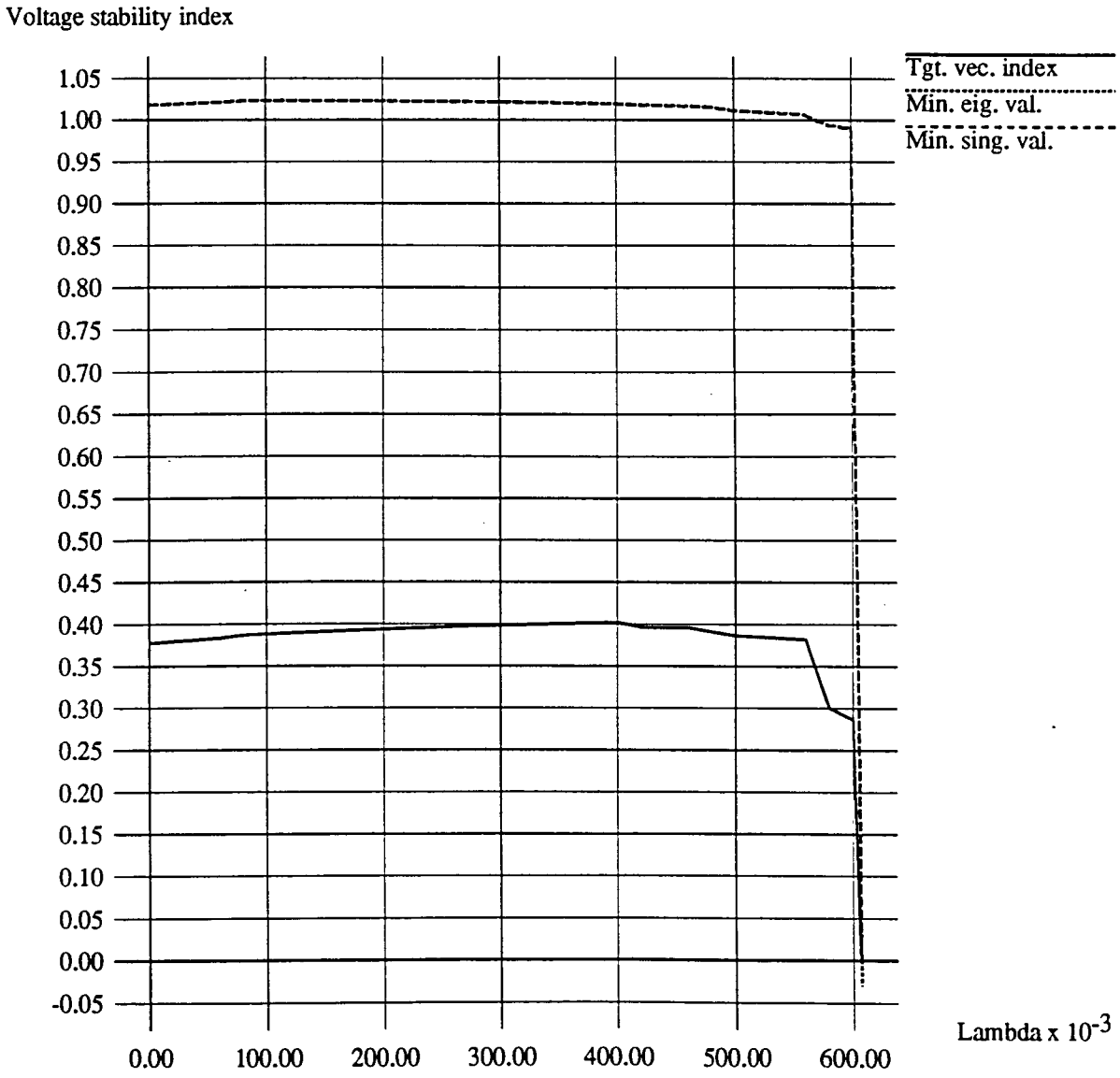

Figure 5.5: Trajectory of voltage stability index, minimum eigenvalue, and minimum singular value

If we look closely at the equation 5.2, for calculating $\frac{dh}{d\lambda}$ we need $\frac{dx}{d\lambda}$, which can be calculated as in equation 2.3 (in our problem, x is the vector of voltage angles and magnitudes). This calculation involves computing the inverse of the Jacobian and fails at the critical point, where the Jacobian is singular and the inverse does not exist. But this $\frac{dx}{d\lambda}$ is given directly by the tangent vector in the continuation power flow. It can be substituted directly in equation 5.2 to obtain the sensitivity of any operating constraint. The next section derives operating constraint sensitivities corresponding to load buses, branches, and generators [32].

5.4.1 Bus sensitivities

For bus sensitivities, the function $h(x, \lambda)$ can be either bus voltage magnitude or angle at a particular bus i. From equation 5.2

$$\frac{dh}{d\lambda} = \sum_{j=1}^{n} \frac{\partial V_i}{\partial x_j}\frac{dx_j}{d\lambda} + \frac{\partial V_i}{\partial \lambda} = \frac{\partial V_i}{\partial V_i}\frac{dV_i}{d\lambda} + 0 = \frac{dV_i}{d\lambda} \tag{5.3}$$

Similarly, if we take bus voltage angle as function h, then

$$\frac{dh}{d\lambda} = \frac{d\delta_i}{d\lambda} \tag{5.4}$$

Close observation of the right-hand sides of the above two equations indicates that the numerators are nothing but the tangent vector elements. Because the value of $d\lambda$ is the same for each dV_i or $d\delta_i$ in a given tangent vector, bus sensitivities are nothing but the tangent vector elements themselves. Bus sensitivities indicate how weak a particular bus is near the critical point and help determine the areas close to voltage instability. The greater the bus sensitivity value the weaker the bus is. Tables 5.1 and 5.2 show the bus sensitivities near the critical point, both according

Table 5.1: Bus sensitivities for the first 10 buses near the critical point - 30-bus system

According to voltage angle		
Bus no.	Tgt. vec. Element	Sensi-tivity
20	0.9465	1.0000
23	0.8805	0.9303
22	0.8774	0.9271
19	0.8710	0.9203
21	0.4959	0.5240
24	0.2923	0.3088
16	0.2609	0.2756
8	-0.1320	0.1394
7	-0.1239	0.1309
4	-0.1014	0.1071

According to voltage magnitude		
Bus no.	Tgt. vec. Element	Sensi-tivity
21	-1.0000	1.0000
24	-0.9391	0.9391
22	-0.9334	0.9334
23	-0.9267	0.9267
16	-0.9149	0.9149
19	-0.9090	0.9090
15	-0.8735	0.8735
20	-0.8696	0.8696
17	-0.6995	0.6995
14	-0.6228	0.6228

to voltage angle and magnitude for the 30-bus test system and for the 17-generator (162-bus) reduced Iowa system, respectively.

5.4.2 Branch sensitivities

Let us consider a branch, ij. Let $V_i\angle\delta_i$ and $V_j\angle\delta_j$ be the voltages at buses i and j, respectively, and let $y_{ij}\angle\theta_{ij}$ be the line admittance. Then the losses in the line ij, neglecting the shunt charging capacitance, can be derived as (see Appendix B):

$$P_{loss} + jQ_{loss} = [V_i^2 + V_j^2 - 2V_iV_jcos(\delta_i - \delta_j)]y_{ij}\angle-\theta_{ij} \tag{5.5}$$

Defining this loss expression as function h, we obtain the sensitivity equation:

$$\begin{aligned}\frac{dh}{d\lambda} &= [(2V_i - 2V_jcos(\delta_i - \delta_j))\frac{dV_i}{d\lambda} + (2V_j - 2V_icos(\delta_i - \delta_j))\frac{dV_j}{d\lambda} \\ &\quad + (2V_iV_jsin(\delta_i - \delta_j))\frac{d\delta_i}{d\lambda} - (2V_iV_jsin(\delta_i - \delta_j))\frac{d\delta_j}{d\lambda}]y_{ij}\angle-\theta_{ij}\end{aligned} \tag{5.6}$$

Table 5.2: Bus sensitivities for the first 10 buses near the critical point - 17-generator system

According to voltage angle		
Bus no.	Tgt. vec. Element	Sensi-tivity
90	-0.6889	1.0000
89	-0.6458	0.9374
86	-0.6073	0.8815
87	-0.5852	0.8494
36	-0.5803	0.8423
56	-0.5638	0.8184
67	-0.5603	0.8133
35	-0.5496	0.7978
104	-0.5477	0.7950
33	-0.5466	0.7934

According to voltage magnitude		
Bus no.	Tgt. vec. Element	Sensi-tivity
63	-1.0000	1.0000
60	-0.9849	0.9849
61	-0.9784	0.9784
58	-0.8883	0.8883
59	-0.8661	0.8661
15	-0.8448	0.8448
62	-0.8445	0.8445
65	-0.8072	0.8072
64	-0.7973	0.7973
10	-0.7729	0.7729

Branch sensitivity indicates how important a particular branch is to voltage stability. Tables 5.3 and 5.4 shows the branch sensitivities obtained near the critical point by considering the Q_{losses} in the branches for the 30-bus test system and for the 17-generator reduced Iowa system respectively. Figures 5.6 and 5.7 show the real power versus total Q_{losses} for ten participating branches (five most and five least). These are the five branches with the highest and the lowest sensitivities for the 30-bus system and for the 17-generator system, respectively. The slope of the curve showing the Q_{losses} in the five most participating branches is steep, compared with that of the five least participating branches. Thus, the rate at which the Q_{loss} in a particular branch is changing is important, but not the magnitude of Q_{loss}. This relation can be observed from the Q_{losses} and the sensitivities from Table 5.3 or 5.4. For example, in Table 5.3, the Q_{loss} in branch 25 is greater than that in branch 3, but branch 3 has a higher sensitivity.

Table 5.3: Branch sensitivities near the critical point for the 30-bus system

Branch no.	Bus i-Bus j	Q losses	Sensitivity
24	16-19	5.4576	1.0000
30	21-22	2.9336	0.5924
32	23-24	2.7159	0.5249
23	16-17	0.9558	0.2377
3	2-3	0.7863	0.1839
25	16-21	1.0473	0.1784
22	15-16	1.3171	0.1541
21	14-15	0.7611	0.1349
33	25-26	0.1217	0.1033
34	26-27	0.5242	0.0807

Table 5.4: Branch sensitivities near the critical point for the 17-generator system

Branch no.	Bus i-Bus j	Q losses	Sensitivity
42	13-62	0.9800	1.0000
196	1-93	1.0729	0.7525
79	25-26	0.2818	0.5245
141	55-149	0.3518	0.4040
154	62-63	0.5018	0.3225
182	84-93	0.3397	0.3174
88	27-126	0.4374	0.2941
152	61-62	0.4807	0.2927
201	95-96	0.3698	0.2902
81	26-74	0.9852	0.2891

These sensitivities provide valuable information for contingency selection. To illustrate, in the 30-bus test system, branch 24, which has the highest sensitivity, is the most critical branch. This can be verified by considering the outage of each branch separately. Outage of branch 24 isolates some part of the system. With the outage of branch 30, we could transfer less power than we could with the outage of branch 32, a fact indicating that branch 30 is more critical than branch 32 for voltage stability. Similarly, for the 17-generator system, with the outage of branch 42, we could transfer less power than with the outage of any other branch. Thus, branch 42 is the system's critical branch in terms of voltage stability.

5.4.3 Generator sensitivities

The reactive power at a generator can be defined as the function h. i.e.,

$$h(x,\lambda) = Q_{Lio} + \lambda \left[K_{L_i} S_{\Delta BASE} sin(\psi_i) \right] + Q_{T_i} \tag{5.7}$$

where

$$Q_{T_i} = \sum_{j=1}^{n} V_i V_j y_{ij} sin(\delta_i - \delta_j - \theta_{ij})$$

with the following definitions

$\mathbf{Q_{L_{io}}}$ = original reactive load,

$\mathbf{K_{L_i}}$ = multiplier designating the rate of load change at bus i as λ changes,

$\psi_\mathbf{i}$ = power factor angle of load change at bus i, and

$\mathbf{S_{\Delta BASE}}$ = apparent power chosen to provide appropriate scaling of λ.

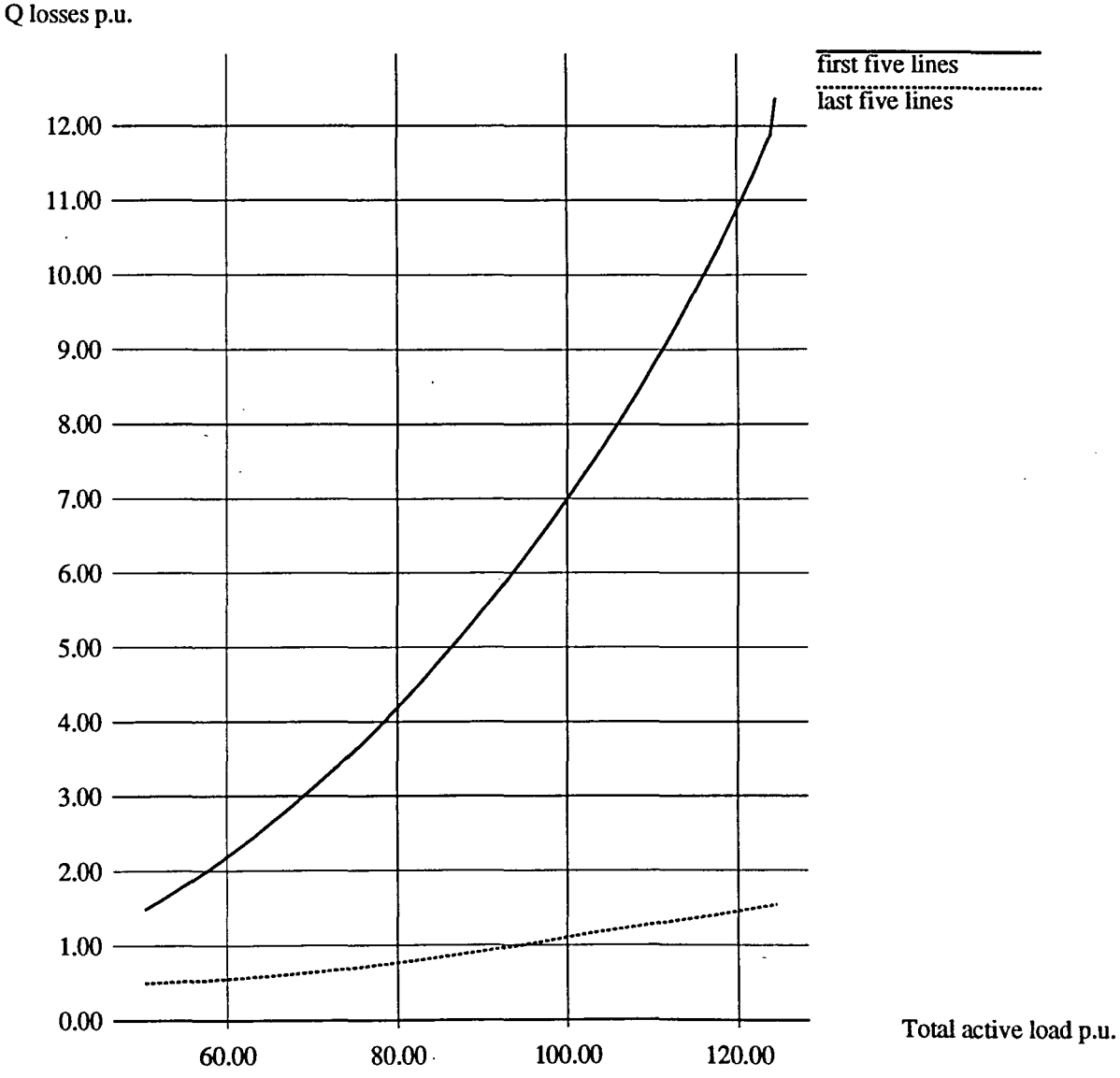

Figure 5.6: Real power versus Q_{losses} curve - 30-bus system

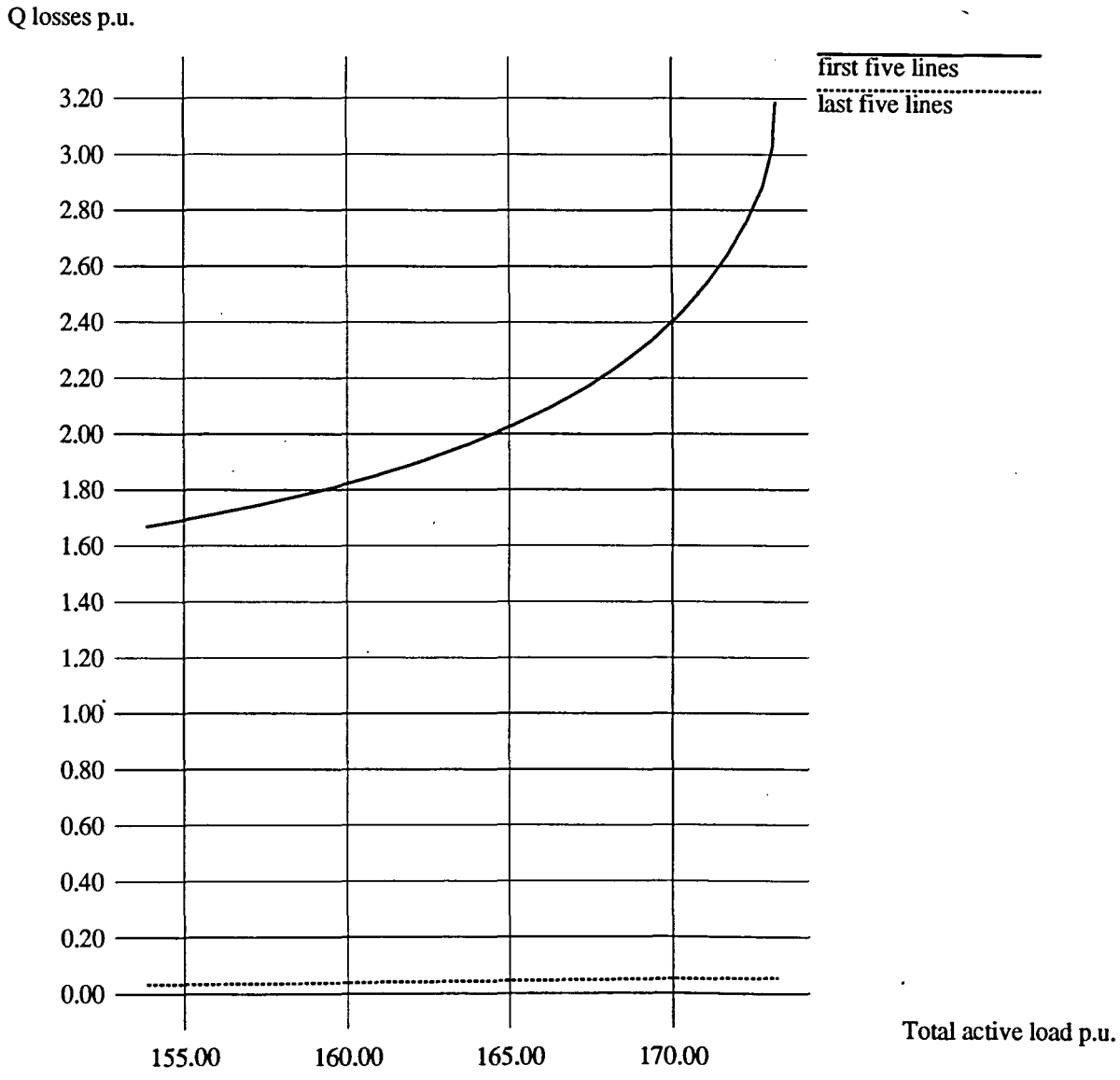

Figure 5.7: Real power versus Q_{losses} curve - 17-generator system

Table 5.5: Generator sensitivities near the critical point for the 30-bus system

Generator no.	Q generation	Sensitivity
29	2.3443	1.0000
25	1.843	0.5318

Table 5.6: Generator sensitivities near the critical point for the 17-generator system

Generator no.	Q generation	Sensitivity
131	1.4013	1.0000
121	2.2922	0.7143
125	2.7090	0.6391
6	2.4771	0.5799
130	1.8297	0.4486
76	4.3247	0.3522

The sensitivity equation therefore becomes

$$\frac{dh}{d\lambda} = \sum_{j=1}^{n} \frac{\partial Q_{T_i}}{\partial x_j} \frac{dx_j}{d\lambda} + K_{L_i} S_{\Delta BASE} sin(\psi_i) \qquad (5.8)$$

Tables 5.5 and 5.6 respectively show the generator sensitivities calculated for the same 30-bus test system and 17-generator reduced Iowa system near the critical point. There are 9 generators in the 30-bus system. Near the critical case only two generators are participating, and the other seven generators already have reached their Q_{limits}. Generator sensitivities indicate those generators that are important in maintaining voltage stability near the critical point. Evidently, generators with high sensitivity are especially important. For example, with the outage of generator 29, we could transfer less power than with the outage of generator 25. These generator sensitivities can be used to obtain a better combination of generators to share the increase in load. Sensitivity results are verified with the finite difference approach.

The sensitivities that we talked about in the above sections are useful not only for finding weak areas in the system, but also for diagnosing modeling deficiencies. In [30], an analysis of voltage stability on the MAPP-MAIN transmission interface of Wisconsin used three different power flow models to determine voltage stability limits. They used bus and branch sensitivities of CPF to assess and compare modeling deficiencies or strengths for three types of power flow models they used. They also used our branch sensitivities to identify the most critical branches in the system, both for normal case and for some contingencies.

CHAPTER 6. CONCLUSIONS AND SUGGESTIONS FOR FUTURE WORK

6.1 Conclusions

The continuation power flow program has been tested on systems as large as 6000 buses and has worked well. A detailed study of load models (constant power; constant current; constant impedance; and composite load, which is a combination of the first three) and their effects on voltage stability also has been conducted. This study defined the concept of load connectivity and clarified the confusion about the critical point with respect to PV curves. The continuation power flow algorithm evidently is not dependent on the type of load model used, but runs with any type of aforementioned load models. The more accurate the load model, the more accurate the results obtained by the method.

The tangent vector information from continuation power flow was used effectively to locate weak areas in the power system, e.g., the buses, branches, and generators that are critical to maintain voltage stability are identified using our proposed sensitivity approach. The branch and generator sensitivities were verified by separately considering outages of the most critical branch and generator. Obviously, with these outages, we were able to transfer less power than with other outages. Even though approaches, such as modal analysis, give the participation information at the base

case, they does not provide much information. In other words, the participation of key components near the base case (especially if remote from the critical point) might be completely different from that of key components near the critical case. The examples included in this work demonstrated the ability of our approach to identify key components in the system with little additional effort.

The sensitivities derived are useful not only for finding weak areas in the system, but also for diagnosing modeling deficiencies. In [30], an analysis of voltage stability on the MAPP-MAIN transmission interface of Wisconsin used three different power flow models to determine the voltage stability limits. The three different models produced three different stability limits. The sensitivity-based CPF successfully identified the most critical branches, both for normal case and for some contingencies. The results were verified by outaging these lines. The authors used the bus and branch sensitivities of CPF to assess and compare modeling deficiencies or strengths for the three types of power flow models used.

6.2 Suggestions for Future Work

Although the continuation power flow has proved practical for the steady-state analysis of voltage stability, there is still room for improvement. Sharing of a system load increase is currently divided according to the initial generation ratio. Now that we have derived the sensitivities of the key generators at each load level, load could be shared according to these factors. We expect more power to be transferred with this type of sharing. In addition when the generator sensitivities are being derived and a particular generator reaches the Q_{limit}, its sensitivity becomes zero. But if we provide more reserve reactive power to this generator, it may become the most

critical generator. So this aspect of Q_{limits} should somehow be taken into account while the generator sensitivities are being derived. One way to do this would be to use reactive power capability curves. The Q_{limits} of the generators, for a given load level and power factor, can be fixed according to these curves, and then the generator senstivities can be computed. Regarding branch sensitivities, the shunt charging capacitance is neglected when the losses in the branches are calculated. If we consider this fact also, increasingly accurate results may be obtained.

An enhancement that would make continuation power flow run faster would be decoupling the Jacobian. Most run time involves the corrector iterations, which require solving $Ax = b$, where A is the Jacobian. So if we use the concept of $P - V$ and $Q - \delta$ decoupling here, it would save memory, simplify calculations, and result in smaller computational times. The decoupling validity, however, should be checked at all load levels until the critical point is reached. To this end, a measure is needed. In [31], the authors came up with a decoupling condition, for which the real and reactive power decoupling is valid (or justifiable). We used this condition as a measure. For the systems we tested, it was valid until the critical point was reached. Moreover, this decoupling measure continuously decreased from the base case to the critical case. Thus, as the system became more stressed, decoupling became less justifiable. Further, checking the condition involves calculating eigenvalues, norms, from which we could not achieve any improvement in cpu time. A more detailed study of decoupling and its application to CPF must be done before definitive conclusions can be reached.

Future studies could involve including the effect of interchange flows in CPF. The independent parameter λ could be related to power import and export to enable

ready assessment of the voltage stability margin in terms of interchange. Finally, the voltage stability problem was examined only from steady-state perspective in this research. Including the capability of accounting for system dynamics will be the future research in this area.

BIBLIOGRAPHY

[1] North American Electric Reliability Council (NERC). *Survey of the Voltage Collapse Phenomenon.* Summary of the Interconnection Dynamics task force's survey on the voltage collapse phenomenon, Aug. 1991.

[2] Tamura, Y., K. Iba, and S. Iwamoto. "Relationship Between Voltage Instability and Multiple Load Flow Solutions in Electric Power Systems." *IEEE Transactions on Power Apparatus and Systems*, vol. PAS-102, pp. 1115-1125, May 1983.

[3] Tamura, Y., K. Iba, and S. Iwamoto. "A Method of Finding Multiple Load Flow Solutions for General Power Systems." A80 043-0, IEEE PES Winter Meeting, Feb. 1980.

[4] Tiranuchit, A., and R. J. Thomas. "A Posturing Strategy against Voltage Instabilities in Electric Power Systems." *IEEE Transactions on Power Systems*, vol. PWRS-3, pp. 87-93, Feb. 1988.

[5] Kessel, P., and H. Glavistch. "Estimating the Voltage Stability of a Power System." *IEEE Transactions on Power Delivery*, vol. PWRD-1, pp. 346-354, July 1986.

[6] Schlueter, R. A., I. Hu, M. W. Chang, J. C. Lo, and A. Costi. "Methods for Determining Proximity to Voltage Collapse." *IEEE Transactions on Power Systems*, vol. PWRS-5, pp. 285-292, 1991.

[7] Iba, K., H. Suzuki, M. Egawa, and T. Watanabe. "Calculation of Critical Loading Condition with Nose Curve Using Homotopy Continuation Method." *IEEE Transactions on Power systems*, vol. PWRS-6, pp. 584-593, May 1991.

[8] Ajjarapu, V., and C. Christy. "The Continuation Power Flow: A Tool for Steady-State Voltage Stability Analysis." *IEEE Transactions on Power Systems*, vol. PWRS-7, pp. 416-423, Feb. 1992.

[9] Task Force on Terms and Definitions, System Dynamic Performance Subcommittee, Power System Engineering Committee. "Proposed Terms and Definitions for Power System Stability." *IEEE Transactions on Power Apparatus and Systems*, vol. PAS-101, pp. 1894-1897, July 1982.

[10] IEEE Working Group. "Voltage Stability of Power Systems: Concepts, Analytical tools, and Industry experience." IEEE 90 TH 0358-2-PWR.

[11] Davidenko, D. "On a New Method of Numerically Integrating a System of Nonlinear Equations." Dokl, Akad, Nauk, USSR, 88, pp. 601-604, 1953.

[12] Seydel, R. *From Equilibrium To Chaos.* New York: Elsevier Science Publishing Co., Inc., 1988.

[13] Moore, G., and A. Spence. "The Calculation of Turning Points of Nonlinear Equations." *SIAM J. Num. Anal.*, vol. 17, pp. 567-576, 1980.

[14] Rheinboldt, W. C., and J. V. Burkhardt. "A Locally Parameterized Continuation Process." *ACM Transactions on Mathematical Software*, vol. 9, no. 2, pp. 215-235, June 1983.

[15] Kubicek, M., and M. Marek. *Computational Methods in Bifurcation Theory and Dissipative Structures.* New York: Springer-Verlag, 1983.

[16] Pai, M. A., and V. Ajjarapu. "Voltage Stability in Power Systems - An Overview." *Proceedings of the Workshop on Recent Advances in Power Systems*, IISc., Bangalore, Aug. 1992.

[17] Ajjarapu, V. "Identification of Steady-State Voltage Stability in Power Systems." *International Journal of Energy Systems*, vol. 11, no. 1, pp. 43-46, 1991.

[18] Alvarado, F. L., and T. H. Jung. "Direct Detection of Voltage Collapse Conditions." *Proceedings: Bulk Power System Voltage Phenomena-Voltage Stability and Security*, Potosi, Missouri, Jan. 1989.

[19] Canizares, C. A., and F. L. Alvarado. "Point of Collapse and Continuation Methods for Large AC/DC Systems." IEEE PES 1992 Winter Meeting, 92 WM 103-2, New York, 1992.

[20] Rheinboldt, W. C. "Solutions Fields of Nonlinear Equations and Continuation Methods." *SIAM J. Num. Anal.*, vol. 19, pp. 653-669, 1989.

[21] Christy, C. D. *Analysis of Steady State Voltage Stability in Large Scale Power Systems.* M.S. Thesis, Iowa State University, Ames, IA, 1990.

[22] General Electric Company. *Load Modeling for Power Flow and Transient Stability Computer studies.* EPRI Publication, EL-5003, vol. 1-4, Jan. 1987.

[23] Sauer, P. W., B. C. Lesieutre, and M. A. Pai. "Dynamic vs. Static Aspects of Voltage Problems." *Proceedings: Bulk Power System Voltage Phenomena Voltage Stability and Security*, International Workshop, Deep Creek Lake, Maryland, Aug. 4-7, 1991.

[24] Schlueter, R. A., A. G. Costi, J. E. Sekerke, and H. L. Forgey. *Voltage Stability and Security Assessment.* EPRI Publication, EL-5967, Aug. 1988.

[25] Gao, B., K. Morison, and P. Kundur. "Voltage Stability Evaluation using Modal Analysis." *IEEE Transactions on Power Systems*, vol. PWRS-7, pp. 1529-1536, Nov. 1992.

[26] Löf, P. A., G. Anderson, and D. J. Hill. "Voltage Stability Indices for Stressed Power Systems." IEEE PES 1992 Winter Meeting, New York, Jan. 26-30, 1992.

[27] Hager, W. W. *Applied Numerical Linear Algebra.* New Jersey: Prentice Hall, Inc., 1988.

[28] Golub, G. H., and C. F. Van Loan. *Matrix Computations.* Baltimore: The Johns Hopkins University Press, 1990.

[29] Frank, P. M. *Introduction to System Sensitivity Theory.* New York: Academic Press, Inc., 1978.

[30] Roddy, R. W., and C. D. Christy. "Voltage Stability on the MAPP-MAIN Transmission Interface of Wisconsin." *Proceedings of the EPRI NERC forum on Voltage Stability*, Breckenridge, Colorado, Sep. 14-15, 1992.

[31] Ilic, M., and A. Stankovic. "Voltage Problems on Transmission Networks Subject to Unusual Power Flow Patterns." 89 WM 158-7, IEEE PES Winter Meeting, New York, Jan. 1988.

[32] Ajjarapu, V., and S. Battula. "Sensitivity Based Continuation Power Flow." *Proceedings of the twenty-fourth annual North American Power Symposium*, Reno, Nevada, Oct. 5-6, 1992.

APPENDIX A. BASIC CONTINUATION METHOD FOR A SIMPLE EXAMPLE

Consider the following simple example with one unknown x

$$f(x,\lambda) = x^2 - 3x + \lambda = 0 \tag{A.1}$$

The Jacobian is

$$\begin{bmatrix} \frac{\partial f}{\partial x} & \frac{\partial f}{\partial \lambda} \end{bmatrix} = [(2x-3) \quad 1]$$

Let the base solution (x_0, λ_0) be $(3,0)$. Then the series of solutions (x_1, λ_1), (x_2, λ_2), $\cdots$ can be found using predictor-corrector continuation as below:

Continuation step 1:

Predictor

To start with, let λ be the continuation parameter. Calculate the tangent vector as below, according to the augmented system given by equation 3.7 (here the index k is 2).

$$\begin{bmatrix} (2x_0 - 3) & 1 \\ 0 & 1 \end{bmatrix} \begin{bmatrix} dx \\ d\lambda \end{bmatrix} = \begin{bmatrix} 0 \\ 1 \end{bmatrix}$$

$$\Rightarrow \begin{bmatrix} 3 & 1 \\ 0 & 1 \end{bmatrix} \begin{bmatrix} dx \\ d\lambda \end{bmatrix} = \begin{bmatrix} 0 \\ 1 \end{bmatrix}$$

$$\Rightarrow dx = \frac{-1}{3} \quad and \quad d\lambda = 1$$

Predict the next solution as

$$\begin{bmatrix} \overline{x}_1 \\ \overline{\lambda}_1 \end{bmatrix} = \begin{bmatrix} x_0 \\ \lambda_0 \end{bmatrix} + \sigma \begin{bmatrix} dx \\ d\lambda \end{bmatrix}$$

where σ is a scalar designating step size (say 0.5).

Thus the predicted solution $(\overline{x}_1, \overline{\lambda}_1)$ becomes $(2.8333, 0.5)$.

Corrector

Correct the predicted solution by solving:

$$-\begin{bmatrix} (2\overline{x}_1 - 3) & 1 \\ 0 & 1 \end{bmatrix} \begin{bmatrix} \Delta x \\ \Delta\lambda \end{bmatrix} = \begin{bmatrix} f(\overline{x}_1, \overline{\lambda}_1) \\ 0 \end{bmatrix}$$

$$\Rightarrow -\begin{bmatrix} 2.6666 & 1 \\ 0 & 1 \end{bmatrix} \begin{bmatrix} \Delta x \\ \Delta\lambda \end{bmatrix} = \begin{bmatrix} 0.0277768 \\ 0 \end{bmatrix}$$

$$\Rightarrow \Delta x = -0.0104165 \quad and \quad \Delta\lambda = 0.$$

Repeat these corrector iterations, until reasonable accuracy is obtained (say $\epsilon = 0.0001$). Now, $\max\{\Delta x, \Delta\lambda\} > \epsilon$. So update $\overline{x}_1$ & $\overline{\lambda}_1$ and repeat the corrector iteration.

$$\Rightarrow \overline{x}_{1_{update}} = \overline{x}_1 + \Delta x = 2.8229164$$
$$\overline{\lambda}_{1_{update}} = \overline{\lambda}_1 + \Delta\lambda = 0.5$$

Corrector iteration:

$$-\begin{bmatrix} (2\overline{x}_{1_{update}} - 3) & 1 \\ 0 & 1 \end{bmatrix} \begin{bmatrix} \Delta x \\ \Delta\lambda \end{bmatrix} = \begin{bmatrix} f(\overline{x}_{1_{update}}, \overline{\lambda}_{1_{update}}) \\ 0 \end{bmatrix}$$

$$\Rightarrow \Delta x = -0.00004075 \quad and \quad \Delta\lambda = 0.$$

Now, $\max\{\Delta x, \Delta\lambda\} < \epsilon$. So stop the corrector iterations. After the first continuation step, the point (x_1, λ_1) is equal to $(2.8228757, 0.5)$.

Continuation step 2:

Select the continuation parameter as the state variable with the largest tangent vector component. i.e.,

$$max\{|dx|, |d\lambda|\} \quad = \quad max\{|-0.333|, |1|\}$$

$\Rightarrow$ continuation parameter is λ and the index k is 2.

Tangent vector:

$$\begin{bmatrix} (2x_1 - 3) & 1 \\ 0 & 1 \end{bmatrix} \begin{bmatrix} dx \\ d\lambda \end{bmatrix} = \begin{bmatrix} 0 \\ 1 \end{bmatrix}$$

$$\Rightarrow dx = -0.3779646 \quad and \quad d\lambda = 1.$$

Predictor (step size is 0.5):

$$\overline{x}_2 = 2.6338934 \quad and \quad \overline{\lambda}_2 = 1.0$$

Corrector:

$$-\begin{bmatrix} 2.26778 & 1 \\ 0 & 1 \end{bmatrix} \begin{bmatrix} \Delta x \\ \Delta\lambda \end{bmatrix} = \begin{bmatrix} 0.035714 \\ 0 \end{bmatrix}$$

$$\Rightarrow \Delta x = -0.0157485 \quad and \quad \Delta\lambda = 0.$$

Now, $\max\{\Delta x, \Delta\lambda\} > \epsilon$. So update $\overline{x}_2$ and $\overline{\lambda}_2$ and repeat corrector iterations, we get $x_2 = 2.618034 \quad and \quad \lambda_2 = 1.0$

Continuation step 3:

For this step also the continuation parameter is λ.

Tangent vector:

$$\begin{bmatrix} (2x_2 - 3) & 1 \\ 0 & 1 \end{bmatrix} \begin{bmatrix} dx \\ d\lambda \end{bmatrix} = \begin{bmatrix} 0 \\ 1 \end{bmatrix}$$

$$\Rightarrow dx = -0.4472 \quad and \quad d\lambda = 1.$$

Predictor (step size is 0.5):

$$\overline{x}_3 = 2.394434 \quad and \quad \overline{\lambda}_3 = 1.5$$

Corrector:

$$-\begin{bmatrix} 1.78887 & 1 \\ 0 & 1 \end{bmatrix} \begin{bmatrix} \Delta x \\ \Delta\lambda \end{bmatrix} = \begin{bmatrix} 0.0500121 \\ 0 \end{bmatrix}$$

$$\Rightarrow \Delta x = -0.027957 \quad and \quad \Delta\lambda = 0.$$

Now, $\max\{\Delta x, \Delta\lambda\} > \epsilon$. So update $\overline{x}_3$ and $\overline{\lambda}_3$ and repeat corrector iterations, we get $x_3 = 2.366026 \quad and \quad \lambda_3 = 1.5$

Continuation step 4:

For this step also the continuation parameter is λ.

Tangent vector:

$$\begin{bmatrix} (2x_3 - 3) & 1 \\ 0 & 1 \end{bmatrix} \begin{bmatrix} dx \\ d\lambda \end{bmatrix} = \begin{bmatrix} 0 \\ 1 \end{bmatrix}$$

$$\Rightarrow dx = -0.57735 \quad and \quad d\lambda = 1.$$

Predictor (step size is 0.5):

$$\overline{x}_4 = 2.07735 \quad and \quad \overline{\lambda}_4 = 2.0$$

Corrector:

$$-\begin{bmatrix} 1.15470 & 1 \\ 0 & 1 \end{bmatrix}\begin{bmatrix} \Delta x \\ \Delta\lambda \end{bmatrix} = \begin{bmatrix} 0.08333 \\ 0 \end{bmatrix}$$

$$\Rightarrow \Delta x = -0.072169 \quad and \quad \Delta\lambda = 0.$$

Now, $\max\{\Delta x, \Delta\lambda\} > \epsilon$. So update $\overline{x}_4$ and $\overline{\lambda}_4$ and repeat corrector iterations, we get $x_4 = 2.000026 \quad and \quad \lambda_4 = 2.0$

Continuation step 5:

For this step also the continuation parameter is λ.

Tangent vector:

$$\begin{bmatrix} (2x_4 - 3) & 1 \\ 0 & 1 \end{bmatrix}\begin{bmatrix} dx \\ d\lambda \end{bmatrix} = \begin{bmatrix} 0 \\ 1 \end{bmatrix}$$

$$\Rightarrow dx = -0.99995 \quad and \quad d\lambda = 1.$$

Predictor:

Now, if we take step size equal to 0.5, the corrector iterations diverge, because the predicted solution is too far from the solution curve. So step size selection plays an important role in the continuation process. If one can select the step size automatically at each step, the speed up of the process improves and solution converges to the required point without any numerical problems. For this example if we take a step size of 0.25 now and continue the process,

$$\overline{x}_5 = 1.75004 \quad and \quad \overline{\lambda}_5 = 2.25$$

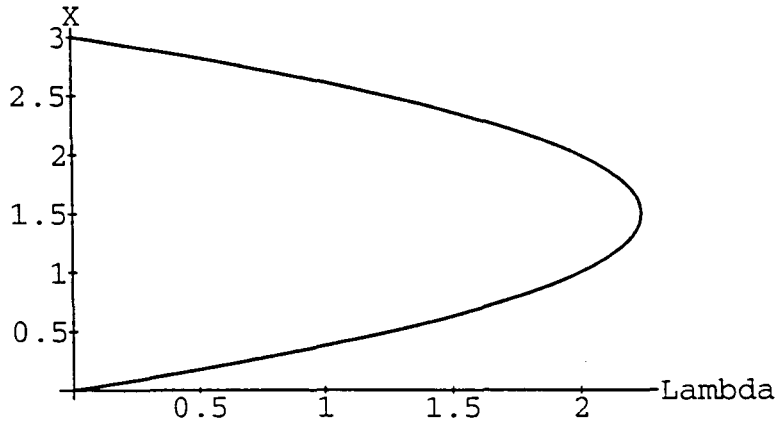

Figure A.1: λ versus x curve

Corrector:

$$-\begin{bmatrix} 0.50008 & 1 \\ 0 & 1 \end{bmatrix}\begin{bmatrix} dx \\ d\lambda \end{bmatrix} = \begin{bmatrix} 0.06252 \\ 0 \end{bmatrix}$$

$$\Rightarrow \Delta x = -0.12502 \quad and \quad \Delta\lambda = 0.$$

Now, $\max\{\Delta x, \Delta\lambda\} > \epsilon$. So update $\overline{x}_5$ and $\overline{\lambda}_5$ and repeat corrector iterations, we get the critical point at:

$$x_5 = 1.5 \quad and \quad \lambda_5 = 2.25$$

Figure A.1 shows the λ versus x curve for the example.

APPENDIX B. DERIVATION OF BRANCH SENSITIVITIES

The following is a derivation of the expression for the branch sensitivities neglecting the shunt charging capacitance.

Let $V_i\angle\delta_i$ and $V_j\angle\delta_j$ be the voltages at buses i and j respectively of the branch ij, and let $y_{ij}\angle\theta_{ij}$ be the line admittance. The current in the branch ij is

$$I_{ij} = \left(V_i\angle\delta_i - V_j\angle\delta_j\right) y_{ij}\angle\theta_{ij}$$

$$\Rightarrow {I_{ij}}^{\star} = \left[(V_i cos\delta_i - V_j cos\delta_j) - j(V_i sin\delta_i - V_j sin\delta_j)\right]$$

Then the total power flow in the branch ij from i to j is given by

$$\begin{aligned}(S_{loss})_{ij} &= (P_{loss})_{ij} + j\,(Q_{loss})_{ij} = V_i {I_{ij}}^{\star} \\ &= [V_i^2 - V_i V_j cos(\delta_i - \delta_j) \\ &\quad -jV_i V_j sin(\delta_i - \delta_j)]y_{ij}\angle -\theta_{ij}\end{aligned}$$

Similarly, the total power flow from j to i is

$$\begin{aligned}(S_{loss})_{ji} &= (P_{loss})_{ji} + j\,(Q_{loss})_{ji} = V_j {I_{ji}}^{\star} \\ &= [V_j^2 - V_i V_j cos(\delta_j - \delta_i) \\ &\quad -jV_i V_j sin(\delta_j - \delta_i)]y_{ij}\angle -\theta_{ij}\end{aligned}$$

The power loss in the branch ij is the algebraic sum of the above two power flows which is

$$P_{loss}+jQ_{loss} = [V_i^2+V_j^2-2V_iV_jcos(\delta_i - \delta_j)]y_{ij}\angle -\theta_{ij}$$

Now differentiating the above loss function w.r.t. λ, we obtain the sensitivity equation as

$$\begin{aligned}\frac{dh}{d\lambda} &= [(2V_i - 2V_jcos(\delta_i - \delta_j))\frac{dV_i}{d\lambda} \\ &\quad + (2V_j - 2V_icos(\delta_i - \delta_j))\frac{dV_j}{d\lambda} \\ &\quad + (2V_iV_jsin(\delta_i - \delta_j))\frac{d\delta_i}{d\lambda} \\ &\quad - (2V_iV_jsin(\delta_i - \delta_j))\frac{d\delta_j}{d\lambda}]y_{ij}\angle -\theta_{ij}\end{aligned}$$